

# On the optimal growth of autocatalytic subnetworks

## A Mathematical Optimization Approach

Víctor Blanco<sup>†,\*</sup>, Gabriel González<sup>†</sup>, and Praful Gagrani<sup>‡</sup>

<sup>†</sup>Institute of Mathematics (IMAG), Universidad de Granada

<sup>\*</sup> Dpt. Quant. Methods for Economics & Business, Universidad de Granada

<sup>‡</sup> Institute of Industrial Science, University of Tokyo

vblanco@ugr.es, ggdominguez@ugr.es, praful@sat.t.u-tokyo.ac.jp

**ABSTRACT.** Chemical reaction networks (CRNs) are essential for modeling and analyzing complex systems across fields, from biochemistry to economics. Autocatalytic reaction networks—networks where certain species catalyze their own production—are particularly significant for understanding self-replication dynamics in biological systems and serve as foundational elements in formalizing the concept of a circular economy. In a previous study, we developed a mixed-integer linear optimization-based procedure to enumerate all minimal autocatalytic subnetworks within a network. In this work, we define the maximum growth factor (MGF) of an autocatalytic subnetwork, develop mathematical optimization approaches to compute this metric, and explore its implications in the field of economics and dynamical systems. We develop exact approaches to determine the MGF of any subnetwork based on an iterative procedure with guaranteed convergence, which allows for identifying autocatalytic subnetworks with the highest MGF. We report the results of computational experiments on synthetic CRNs and two well-known datasets, namely the Formose and E. coli reaction networks, identifying their autocatalytic subnetworks and exploring their scientific ramifications. Using advanced optimization techniques and interdisciplinary applications, our framework adds an essential resource to analyze complex systems modeled as reaction networks.

### 1. INTRODUCTION

Computational Optimization offers a wide range of modeling and solution techniques capable of addressing questions that arise across diverse scientific disciplines by simulating and designing complex systems observed in nature (see, e.g., Banga, 2008; Fromer and Coley, 2024; Naseri and Koffas, 2020). Among the many families of Mathematical Optimization problems, Network Optimization stands out for its tangible practical applications. A network is a structure comprising a set of interconnected entities (nodes) connected through links (edges). Network Optimization focuses on optimizing objectives related to these network structures (see Balakrishnan, 2019, and references therein).

Network Optimization tools are widely applied in fields such as logistics, transportation, and telecommunications, where complex interactions among the entities are represented as physical links in the network (Cordeau et al., 2006; Frost and

Melamed, 1994; Hearnshaw and Wilson, 2013) or virtual links representing interactions between observations in a dataset (Benati et al., 2023). Identifying network substructures with specific properties or optimizing network design is crucial in many fields. Fundamental problems in network design include shortest paths (Schrijver, 2012), minimum spanning trees (Graham and Hell, 1985), Steiner trees (Hwang and Richards, 1992), and Hamiltonian graphs (Bermond, 1979).

In this work, we examine pivotal problems in Chemical Reaction Networks (CRNs) through the lens of optimization, demonstrating how certain scientific questions can be addressed using Network Optimization techniques. Specifically, we focus on the challenging problem of understanding the existence and limits to the growth of self-replicating or autocatalytic subnetworks. As we explain below, these subnetworks are critical for explaining the emergence and maintenance of complexity in chemical and biological systems and have significant applications in fields such as economics.

CRNs provide a general framework for describing complex systems in which various species interact, reacting and transforming into other species (Baez and Pollard, 2017). Analyzing CRNs has significant implications across several scientific fields, including dynamical systems, biochemistry, ecology, epidemiology, economics, and the study of life’s origins (see, e.g., Feinberg, 2019; Avram et al., 2024; Smith and Morowitz, 2016; Peng et al., 2020, among others). Topologically, CRNs can be represented as directed multi-hypergraphs (Andersen et al., 2021), making them an indispensable tool for modeling various aspects of complex systems. In chemistry, the nodes and directed hyperedges correspond to molecular species and chemical reactions, but the framework also extends to representing organisms and interactions in ecology or goods and industries in economics (see Table 1). The study of CRNs is particularly important for understanding the origins of life, as these structures offer insights into the transition from chemistry to biology (Dill and Agozzino, 2021; Kocher and Dill, 2023).

<b>Hypergraphs</b>	<b>CRN</b>	<b>Economics</b>
Vertices	Species	Goods
Hyperedges	Reactions	Industries
0-cochain	Chemical potentials	Prices of goods
1-cochain	Reaction flow vector	Industrial operation intensities

TABLE 1. Dictionary between hypergraphs (Kobayashi et al., 2023), CRNs (Feinberg, 2019), and economics (von Neumann, 1945).

Among the intricate structures found in CRNs, autocatalytic subnetworks stand out as particularly intriguing for several reasons. Autocatalysis refers to a process in which a series of reactions results in an increase in specific species, known as autocatalysts, provided these species are already present (Blokhuis et al., 2020). This concept generalizes biological self-replication and plays a crucial role in understanding chemical evolution (Bagley et al., 1992; Szathmáry, 2006). In economics, autocatalysis captures the essence of a growing circular economy, where goods are

produced from other goods while generating a net surplus. Autocatalytic subnetworks help elucidate self-organizing systems by identifying subsets of reactions that enable the generation and persistence of the entire network (Peng et al.). Mathematically, these subnetworks are shown to exhibit positive feedback (Vassena and Stadler, 2024), and their thermodynamic implications have been explored in Depons et al. (2024); Kosci et al. (2024).

Identifying autocatalytic subnetworks (and their corresponding autocatalytic species) within a CRN is a well-known challenge, as the problem is NP-complete (Andersen et al., 2012; Weller-Davies et al., 2020; Kosci et al., 2024), presenting significant mathematical and computational difficulties. Blokhuis et al. (2020) introduced a mathematical framework for autocatalysis based on the stoichiometric matrix of the CRN. More recently, tools have been developed to detect and enumerate autocatalytic subnetworks using (discrete) mathematical optimization approaches (Peng et al.; Gagrani et al., 2024). These studies demonstrated that even small CRNs can contain a vast number of minimal autocatalytic subnetworks. However, the growth properties of these subnetworks have not yet been rigorously analyzed. The present work, to our knowledge, provides the first comprehensive study of these properties from both mathematical and computational perspectives. It introduces a method to prioritize the detection of autocatalytic subnetworks based on their growth factors and to rank autocatalytic subnetworks identified through other approaches.

In this paper, we define a measure for a subnetwork’s optimal ability to produce more than it consumes: the *maximum growth factor*. This measure extends the economic production model introduced by von Neumann (1945). We show that this factor, under autonomy conditions, is always greater than 1 for an autocatalytic subnetwork and develop a mathematical optimization framework to numerically compute its exact value for a given CRN subnetwork using a Dinkelbach-type procedure (Crouzeix et al., 1985). First, we study a simplified scenario where the subnetwork and its self-replicating species are predefined. This leads to a continuous non-convex optimization problem solvable via generalized fractional programming. Next, we address the case where the subnetwork is given, but the self-replicating species are unknown. Here, the optimization problem involves determining both the growth factor and the optimal set of self-replicating species, requiring a discrete solution strategy using a branch-and-bound approach. Finally, we propose a comprehensive framework to construct a subnetwork maximizing the growth factor. This framework not only identifies the autocatalytic subnetwork but also lists the relevant reactions and species. Additionally, we demonstrate how this framework can be adapted to impose constraints, such as specifying species to be consumed, produced, or self-replicating, as categorized in Gagrani et al. (2024).

Our proposal enables the detection and computation of autocatalytic subnetworks with significantly less effort than previous approaches in the literature. The validation of our proposal is performed with two studies. First, we computationally validate our approach by reporting the results of an extensive battery of computational experiments on synthetic (but still realistic) CRNs generated using the methodology proposed in (Kochen et al., 2022). Secondly, we apply our methods

to two well-known CRNs: the *Formose* reaction network and the *E. coli* metabolism network. For these networks, we obtained, within a reasonable CPU time, the subnetworks that maximize the MGF (Figure 1), which were found to be autocatalytic subnetworks. We conclude with a summary of our contributions and discuss potential scientific applications as well as computational extensions of our research for future studies.

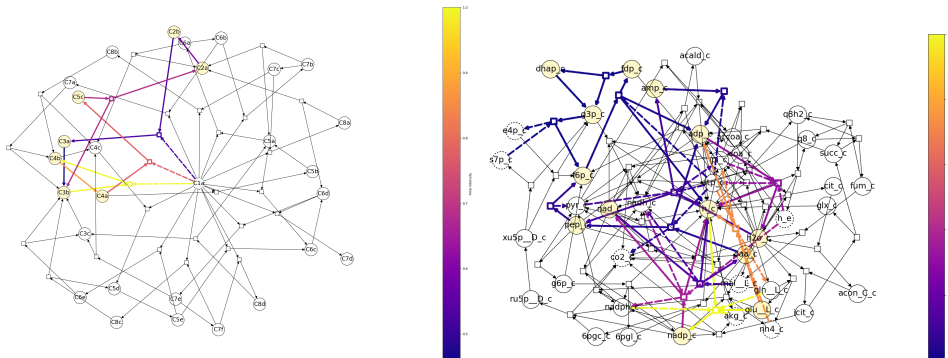


FIGURE 1. Autonomous subnetworks with the highest MGF are shown for the *Formose* network (above) and the *E. coli metabolism* (below). The legends indicate the optimal flow-intensity assignment for each reaction in the subnetwork.

## 2. METHODS

Chemical Reaction Networks (CRNs) provide a highly expressive and versatile framework for modeling inter-species interactions and analyzing their resulting dynamics (Clarke, 1988; Veloz et al., 2014; Feinberg, 2019). A CRN is considered autocatalytic within a set if it consumes all the species in that set while producing even more of them. Autocatalysis is a crucial property of CRNs, essential for formalizing concepts of reproduction in ecological and biological applications (Peng et al., 2022). In this section, following the approach by Gagrani et al. (2024), we introduce the notation and review the main components necessary for the developments in this paper.

We adopt the following definition of chemical reaction networks (Hirono et al., 2021).

A CRN can be identified with a directed multi-hypergraph specified by the quadruple  $\mathcal{G} = (\mathcal{S}, \mathcal{R}, s, t)$ , where:

- $\mathcal{S}$  is the vertex set, that are usually called *species* of the CRN,
- $\mathcal{R}$  is the set of hyperedges, which is identified as the *reactions* of the CRN, and
- $s$  and  $t$  are source and target functions,  $s : \mathcal{R} \rightarrow \mathbb{Z}_+^{\mathcal{S}}$  and  $t : \mathcal{R} \rightarrow \mathbb{Z}_+^{\mathcal{S}}$ , which specify the reactants and products of a reaction, respectively (here,  $\mathbb{Z}_+$  stands for the set of nonnegative integers, and  $\mathbb{Z}_+^{\mathcal{S}}$  are all the mappings

from  $\mathcal{S}$  to  $\mathbb{N}$ , also known as *complexes* (Feinberg, 2019)). For each reaction,  $r \in \mathcal{R}$ , its source,  $s(r)$ , and target,  $t(r)$ , are referred to as its *input and output complex*, respectively.

Given a CRN,  $\mathcal{G} = (\mathcal{S}, \mathcal{R}, s, t)$ , we define a matrix-pair  $(\mathbb{S}^-, \mathbb{S}^+)$  of  $\mathcal{S} \times \mathcal{R}$  matrices, termed the *input-output stoichiometric matrices*, as follows:

$$\mathbb{S}_{sr}^- := s(r)(s), \quad \mathbb{S}_{sr}^+ := t(r)(s), \quad s \in \mathcal{S}, r \in \mathcal{R}. \quad (1)$$

Using these input and output matrices, each reaction  $r \in \mathcal{R}$  can be equivalently written as:

$$r : \sum_{s \in \mathcal{S}} \mathbb{S}_{sr}^- s \rightarrow \sum_{s \in \mathcal{S}} \mathbb{S}_{sr}^+ s,$$

indicating that the input complex of  $r$  (combinations of the species in  $\mathcal{S}$  with the coefficients in  $\mathbb{S}_{sr}^-$  for  $s \in \mathcal{S}$ ) results in the output complex of  $r$  (combinations of the species in  $\mathcal{S}$  with the coefficients in  $\mathbb{S}_{sr}^+$  for  $s \in \mathcal{S}$ ), and we can equivalently specify a CRN by the quadruple  $(\mathcal{S}, \mathcal{R}, \mathbb{S}^-, \mathbb{S}^+)$  or, abusing of notation, by the pair  $\mathcal{G} = (\mathcal{S}, \mathcal{R})$ . The difference  $\mathbb{S} = \mathbb{S}^+ - \mathbb{S}^-$  is called the (net) *stoichiometric matrix* of the chemical reaction network  $\mathcal{G}$  and specifies the incidence matrix of the directed multi-hypergraph (Hirono et al., 2021).

We say that  $\mathcal{G}' = (\mathcal{S}', \mathcal{R}')$  is a *subnetwork* of a CRN  $\mathcal{G} = (\mathcal{S}, \mathcal{R})$ , and will be denoted as  $\mathcal{G}' \subseteq \mathcal{G}$ , if  $\mathcal{R}' \subseteq \mathcal{R}$  and all the species that appear in the input or output complexes in  $\mathcal{R}'$  are in  $\mathcal{S}'$ .

Each nonnegative vector  $\mathbf{x} \in \mathbb{R}_+^{\mathcal{R}} \setminus \{\mathbf{0}\}$  can be identified with a flow that (linearly) combines the reactions in  $\mathcal{R}$  and results in a net amount of species consumed and others produced by this combination. Specifically, the products  $\mathbb{S}^- \mathbf{x}, \mathbb{S}^+ \mathbf{x} \in \mathbb{R}^{\mathcal{S}}$ , are the vectors of amounts of species *consumed* and *produced* under the flow vector  $\mathbf{x}$ , respectively.

Observe that, denoting the species population vector as  $\nu \in \mathbb{N}^{\mathcal{S}}$ , the net change vector in the amount of species  $\Delta\nu$  under a flow  $\mathbf{x}$  is  $\Delta\nu = \mathbb{S}\mathbf{x}$ .

Given a subnetwork  $\mathcal{G}' \subseteq \mathcal{G}$  of a CRN, and  $\mathcal{M} \subset \mathcal{S}'$ , the restriction of  $\mathcal{G}'$  to the species in  $\mathcal{M}$  is called a *motif* and denoted as  $\mathcal{G}'|_{\mathcal{M}}$ . The main notion that motivates this work is that of an autocatalytic subnetwork which is introduced as follows.

**Definition 1.1** (Autocatalytic subnetwork). *A subnetwork  $\mathcal{G}' = (\mathcal{S}', \mathcal{R}', \mathbb{S}^-, \mathbb{S}^+) \subseteq \mathcal{G}$  is **autocatalytic** in the set  $\mathcal{M} \subseteq \mathcal{S}'$  if it satisfies:*

- (1) *Every reaction produces and consumes at least one species in the autocatalytic set, and every autocatalytic species is produced and consumed by at least one reaction:*

$$\forall r \in \mathcal{R}', \exists s, s' \in \mathcal{M} : \mathbb{S}_{sr}^+ > 0, \mathbb{S}_{s'r}^- > 0, \quad (\text{A}^r)$$

$$\forall s \in \mathcal{M}, \exists r, r' \in \mathcal{R}' : \mathbb{S}_{sr}^+ > 0, \mathbb{S}_{sr'}^- > 0. \quad (\text{A}^s)$$

*These conditions are known as reaction autonomy and species autonomy, respectively. The verification of both conditions is termed as **autonomy** of the subnetwork.*

- (2) *There exists a semi-positive flow such that the net production of all autocatalytic species is strictly positive,*

$$\exists \mathbf{x} \in \mathbb{R}_{>0}^{\mathcal{R}'} : \sum_{r \in \mathcal{R}'} \mathbb{S}_{sr} \mathbf{x}_r > 0 \quad \forall s \in \mathcal{M}. \quad (\text{P})$$

*This condition is usually known as **productivity** of the subnetwork.*

The set  $\mathcal{M}$  in the above definition is called the set of *autocatalytic species* of the autocatalytic subnetwork  $\mathcal{G}'$ .

Our definition of autocatalysis closely follows the one by Blokhuis et al. (2020) where  $\mathcal{G}'|_{\mathcal{M}}$  is named an *autocatalytic motif*. A motif is said **minimally autocatalytic** if it does not contain a proper autocatalytic subnetwork. The stoichiometric matrix of a minimally autocatalytic subnetwork,  $\mathbb{S}|_{\mathcal{M}, \cdot}$ , is called an **autocatalytic core** (AC).

Mathematical properties of ACs and their role from a dynamical systems perspective is investigated by Vassena and Stadler (2024). The enumeration of the set of ACs is known to be a challenging problem that can be addressed using Integer Optimization (see Peng et al.; Gagrani et al., 2024).

**Maximum Growth Factor (MGF).** In this section, we explore the dynamics of a CRN or one of its subnetworks, introduce the concept of its *maximum growth factor* (MGF), and present a mathematical optimization approach to compute this metric. Our definition of the MGF is closely related to the technological expansion rate introduced by von Neumann (1945), reviewed in (Gale, 1989, Ch. 9.5).

Consider a CRN  $\mathcal{G} = (\mathcal{S}, \mathcal{R})$  modeled as a discrete-time dynamical system, where a time index  $t$  is associated with the reaction flow vector  $\mathbf{x} \in \mathbb{R}_+^{\mathcal{R}}$ . At any time  $t$ , an autocatalytic subnetwork  $\mathcal{G}' = (\mathcal{S}', \mathcal{R}')$  operating under a productive flow  $\mathbf{x}(t)$  generates more of the species in the autocatalytic set  $\mathcal{M}$  than it consumes, that is:

$$\mathbb{S}_{sr}^+ \mathbf{x}(t)_r > \mathbb{S}_{sr}^- \mathbf{x}(t)_r, \forall s \in \mathcal{M}, r \in \mathcal{R}'.$$

For simplicity, we denote the input and output stoichiometric submatrices, restricted to the species in  $\mathcal{M}$ , by  $\overline{\mathbb{S}}^-$  and  $\overline{\mathbb{S}}^+$ , respectively, for the remainder of this subsection.

In this system, production at time  $t$  serves as the input for time  $t+1$ . Hence, the inequalities above suggest that at time  $t+1$ , a greater reaction flow vector can be chosen, while still using the resources produced in the previous step:

$$\overline{\mathbb{S}}^+ \mathbf{x}(t) \geq \overline{\mathbb{S}}^- \mathbf{x}(t+1). \quad (2)$$

Additionally, if we require the relative proportions of the reaction flows in  $\mathbf{x}(t+1)$  to remain the same as in  $\mathbf{x}(t)$ , preserving the structure of the dynamics,  $\mathbf{x}(t+1)$  must be a scalar multiple of  $\mathbf{x}(t)$  by a constant factor  $\alpha$ , referred to as the growth factor:

$$\mathbf{x}(t+1) = \alpha \mathbf{x}(t). \quad (3)$$

Substituting this into equation (2) leads to the condition:

$$\overline{\mathbb{S}}^+ \mathbf{x}(t) \geq \alpha \overline{\mathbb{S}}^- \mathbf{x}(t). \quad (4)$$

We say that the subnetwork  $\mathcal{G}'$  with initial flow  $\mathbf{x}(0)$  is expanding if  $\alpha \geq 1$ , and contracting if  $\alpha < 1$ .

The focus of this paper is the analysis of how to determine initial flows that induce maximal expansion in the system.

**Definition 1.2** (Maximum Growth Factor (MGF)). *Let  $\mathcal{G} = (\mathcal{S}, \mathcal{R})$  be a CRN,  $\mathcal{G}' = (\mathcal{S}', \mathcal{R}') \subseteq \mathcal{G}$ ,  $\emptyset \neq \mathcal{M} \subset \mathcal{S}'$ , and  $\mathbf{x} \in \mathbb{R}_{>0}^{\mathcal{R}}$  a flow. The growth factor of  $\mathcal{G}'$  for  $\mathbf{x}$  is defined as:*

$$\alpha(\mathcal{G}', \mathcal{M}; \mathbf{x}) = \inf_{s \in \mathcal{M}} \frac{\sum_{r \in \mathcal{R}'} \mathbb{S}_{sr}^+ \mathbf{x}_r}{\sum_{r \in \mathcal{R}'} \mathbb{S}_{sr}^- \mathbf{x}_r},$$

that represents the production rate of the subnetwork for the initial flow  $\mathbf{x}$ , indicating the smallest value of  $\alpha$  in (4) that can be achieved for  $\mathbf{x}$ . Since realistic flows require  $\mathbf{x} \neq \mathbf{0}$  and  $\mathbb{S}^-$  is a nonzero, nonnegative integer matrix, the above infimum can be replaced with a minimum.

The **Maximum Growth Factor (MGF)** of  $\mathcal{G}'$  over  $\mathcal{M}$  is the maximum value for the growth factor above that can be achieved for any flow  $\mathbf{x} \in \mathbb{R}_+^{\mathcal{R}}$ :

$$\alpha(\mathcal{G}', \mathcal{M}) = \max_{\mathbf{x} \in \mathbb{R}_{>0}^{\mathcal{R}}} \alpha(\mathcal{G}', \mathcal{M}; \mathbf{x}).$$

This value coincides with the maximum value of  $\alpha$  that satisfies equation (4).

In this work, we present a mathematical framework to compute this rate and analyze its implications for identifying autocatalytic subnetworks. The primary tool used in this study is *Mathematical Optimization*.

The maximum growth factor of a subnetwork  $\mathcal{G}'$  can be formulated as the following mathematical optimization problem:

$$\begin{aligned} \alpha(\mathcal{G}', \mathcal{M}) &:= \max \alpha \\ \text{s.t.} \quad & \overline{\mathbb{S}^+} \mathbf{x} \geq \alpha \overline{\mathbb{S}^-} \mathbf{x}, \\ & \overline{\mathbb{S}^-} \mathbf{x} \geq \mathbf{1}, \\ & \mathbf{x} \in \mathbb{R}_+^{\mathcal{R}'}, \alpha \geq 0. \end{aligned} \tag{MGF}$$

Therefore, the MGF can be interpreted as a robust choice of flow that maximizes the minimum growth factor among the species in the system.

A key contribution of this paper is the development of novel computational strategies to improve the analysis of autocatalytic networks using the MGF. In the following, we present one of the main results of this paper, which serves as a foundation for the remainder of the study. This result establishes a *link* between the MGF and the autocatalysis of a chemical subnetwork. Specifically, we prove that the MGF can act as a certificate of autocatalysis for a subnetwork.

**Theorem 1.** *Let  $\mathcal{G} = (\mathcal{S}, \mathcal{R})$  a CRN,  $\mathcal{G}' = (\mathcal{S}', \mathcal{R}') \subseteq \mathcal{G}$ , and  $\emptyset \neq \mathcal{M} \subset \mathcal{S}'$ . Then, if  $\mathcal{G}'$  is autocatalytic in  $\mathcal{M}$ , then  $1 < \alpha(\mathcal{G}', \mathcal{M}) < \infty$ . Furthermore, if  $\mathcal{G}'$  is autonomous and  $\alpha(\mathcal{G}', \mathcal{M}) > 1$ , then  $\mathcal{G}'$  is autocatalytic.*

*Proof.* The result follows from Lemmas 2 and 3. □

**Computation of MGF.** In this subsection, we address the computational aspects of determining the MGF. The problem (MGF) is neither convex nor concave, and thus, standard convex optimization tools are not directly applicable. However, the MGF can also be formulated as a generalized fractional programming problem, which is computationally challenging (e.g., Barros et al. (1996); Blanco et al. (2013); Crouzeix and Ferland (1991)). To solve (MGF), we adapt a Dinkelbach-type procedure (e.g., Crouzeix and Ferland (1991)), which iteratively computes  $\alpha(\mathcal{G}', \mathcal{M})$  and guarantees convergence to the actual value.

In what follows we analyze the computation of the MGF, for a given subnetwork,  $\mathcal{G}' = (\mathcal{S}', \mathcal{R}')$ , and a given set  $\mathcal{M} \subseteq \mathcal{S}'$ . A specific instance of this occurs when  $\mathcal{S}' = \mathcal{M}$ , meaning all species in the subgraph are potential autocatalytic species.

The algorithm that we propose for computing the MGF, whose pseudocode is detailed in Algorithm 1, is based on solving, exactly, the mathematical optimization model in MGF by applying an ad-hoc Dinkelbach-type procedure to solve it. Specifically, we begin by initializing the flow vector to  $\mathbf{x}_0$ . For each flow vector obtained during the procedure, we compute the growth factor induced by that flow, denoted as  $\alpha_{\text{it}}$ . Next, we solve an auxiliary linear program to compute the optimal values  $\rho$  and  $\mathbf{x}_{\text{it}}$ . If  $\rho = 0$ , the current solution is optimal, and the growth factor for this flow,  $\alpha_{\text{it}}$ , corresponds to the MGF. If not, the flow vector is updated based on the solution of the linear program, and the process is repeated. A pseudocode for our proposed algorithm is detailed in Algorithm 1. The convergence of this procedure is guaranteed by Crouzeix et al. (1985).

When the set  $\mathcal{M}$  is either unknown or not all species in the subnetwork satisfy the conditions for autocatalysis, determining this set becomes an integral part of the decision-making process for computing the growth factor. In this case, the set  $\mathcal{M}$  must be constructed as part of the procedure. The goal of this section is to outline a method for computing the set  $\mathcal{M}$  that maximizes the growth factor for a given subnetwork  $\mathcal{G}'$ , with the input and output stoichiometric matrices denoted by  $\overline{\mathbb{S}}^-$  and  $\overline{\mathbb{S}}^+$ , respectively.

The primary challenge in this problem lies in not only calculating the growth factor via its optimal flow but also selecting the optimal subset  $\mathcal{M} \subseteq \mathcal{S}'$  from among  $2^{|\mathcal{S}'|}$  possible combinations—a task that is both computationally intensive and impractical to enumerate exhaustively. Furthermore, since the ultimate aim is to construct autocatalytic subnetworks, the set  $\mathcal{M}$  must satisfy two key conditions:

- (1)  $\mathcal{M} \neq \emptyset$  (to avoid an infinite growth factor), and
- (2) every species in  $\mathcal{M}$  must be both consumed and produced.



Given these constraints, the problem can be formally written as:

$$\begin{aligned}
\alpha(\mathcal{G}') &:= \max_{\mathcal{M} \subseteq \mathcal{S}'} \alpha \\
\text{s.t. } & (\overline{\mathbb{S}^+})_s \mathbf{x} \geq \alpha (\overline{\mathbb{S}^-})_s \mathbf{x}, & \forall s \in \mathcal{M}, \\
& (\overline{\mathbb{S}^-})_s \mathbf{x} \geq 1, & \forall s \in \mathcal{M}, \\
& \sum_{r \in \mathcal{R}'} \overline{\mathbb{S}^+}_{sr} \geq 1, & \forall s \in \mathcal{M}, \\
& \sum_{r \in \mathcal{R}'} \overline{\mathbb{S}^-}_{sr} \geq 1, & \forall s \in \mathcal{M}, \\
& \mathbf{x} \in \mathbb{R}_+^{\mathcal{R}'}, \alpha \geq 0.
\end{aligned} \tag{5}$$

where  $(\overline{\mathbb{S}^-})_s$  and  $(\overline{\mathbb{S}^+})_s$  refer to the  $s$ -th rows of the input and output stoichiometric matrices, respectively.

Note that in the mathematical model described above, the set  $\mathcal{M}$  is unknown (is part of the decisions to be made), and then the matrices  $(\overline{\mathbb{S}^-})$  and  $(\overline{\mathbb{S}^+})$ . To incorporate this decision of whether or not a species belongs to  $\mathcal{M}$ , we introduce the binary decision variable:

$$a_s = \begin{cases} 1 & \text{if } s \in \mathcal{M}, \\ 0 & \text{otherwise} \end{cases} \quad \forall s \in \mathcal{S}'.$$

Using this notation, the resulting submatrices  $(\overline{\mathbb{S}^-})$  and  $(\overline{\mathbb{S}^+})$ , can be written in terms of the  $a$ -variables as  $(\overline{\mathbb{S}^-}) = A\mathbb{S}^-$  and  $(\overline{\mathbb{S}^+}) = A\mathbb{S}^+$ , respectively, where  $A$  is the binary matrix that results from removing the rows of the  $|\mathcal{S}|$ -identiy matrix the rows with zero  $a$ -values.

The problem can be then equivalently formulated as a suitable mathematical optimization problem:

$$\begin{aligned}
& \max \alpha \\
\text{s.t. } & \mathbb{S}_s^+ \mathbf{x} \geq \alpha a_s \mathbb{S}_s^- \mathbf{x}, & \forall s \in \mathcal{S}', \\
& \mathbb{S}_s^- \mathbf{x} \geq a_s, & \forall s \in \mathcal{S}', \\
& \sum_{s \in \mathcal{S}'} a_s \geq 1, \\
& a_s \in \{0, 1\}, & \forall s \in \mathcal{S}', \\
& \mathbf{x} \in \mathbb{R}_+^{\mathcal{R}'}, \alpha \geq 0.
\end{aligned}$$

Note that the first set of constraints indicates that if  $a_s = 1$ , then the growth factor for the  $s$ -th species is accounted for the whole growth factor, but in case  $a_s = 0$ , then the constraint is redundant, so  $\alpha$  (the growth factor) is not restricted. Then, to avoid solutions where all species take  $a_s = 0$ , we enforce the solutions to verify that at least one species must take value  $a_s = 1$ .

The pseudocode for this procedure is provided in Algorithm 2, whose convergence is also guaranteed.

The final, and most innovative, methodological contribution of this paper, is mathematical model that we propose to construct autocatalytic subnetworks with the maximal possible growth factor. To achieve this, we develop a mathematical optimization-based framework with two main objectives:

- (1) to identify an autonomous subnetwork that maximizes the growth factor among all possible subnetworks, and
- (2) to determine whether the entire CRN contains an autocatalytic subnetwork.

By combining these elements, we can compute the optimal autonomous growth factor subnetwork for a given CRN. This approach, in conjunction with the algorithms presented by Gagrani et al. (2024), would allow the construction of a set of autocatalytic subnetworks sorted by their growth rates.

Given a CRN,  $\mathcal{G} = (\mathcal{S}, \mathcal{R})$ , our goal is to construct a subnetwork  $\mathcal{G}' = (\mathcal{S}', \mathcal{R}')$  and a set of *potential autocatalytic* species  $\mathcal{M} \subset \mathcal{S}$  that maximizes the growth factor. By Theorem 1, in case the obtained subnetwork has a growth factor greater than or equal to one, it is considered autocatalytic and the set  $\mathcal{M}$  would be a proper autocatalytic set of species. Otherwise, if no autocatalytic subnetwork is found, the subnetwork with the highest growth factor is computed, but the set  $\mathcal{M}$  will be an autonomous set of species although not productive (none of the subset of species is).

We propose a mathematical optimization approach for constructing such a subnetwork. The proposed mathematical program uses the decision variables listed in the following table which are identified with the four main decisions to be made. These variables include those determining which species are included in the subnetwork  $\mathcal{G}'$  ( $y$ ), which species are in  $\mathcal{M}$  ( $a$ ), which reactions are used in  $\mathcal{G}'$  ( $z$ ), the growth factor for the subnetwork ( $\alpha$ ), and the flow vector ensuring the growth factor ( $\mathbf{x}$ ).

$a_s = \begin{cases} 1 & \text{if species } s \text{ is in } \mathcal{M} \\ 0 & \text{otherwise} \end{cases} \quad \text{for } s \in \mathcal{S}.$ $z_r = \begin{cases} 1 & \text{if } r \text{ is in } \mathcal{R}' \\ 0 & \text{otherwise} \end{cases} \quad \text{for } r \in \mathcal{R}.$ $\mathbf{x} \in \mathbb{R}_+^{ \mathcal{R} } : \text{flow vector.}$ $\alpha \in \mathbb{R}_+ : \text{growth factor.}$
--

These variables are combined through the following inequalities to ensure the adequate construction of the desired subnetwork:

- The growth factor is well-defined:

$$\sum_{r \in \mathcal{R}} \mathbb{S}_{sr}^+ z_r \mathbf{x}_r \geq \alpha a_s \sum_{r \in \mathcal{R}} \mathbb{S}_{sr}^- z_r \mathbf{x}_r, \quad \forall s \in \mathcal{S}. \quad (6)$$

- The set  $\mathcal{M}$  is not empty:

$$\sum_{s \in \mathcal{S}} a_s \geq 1. \quad (7)$$

- The denominator in the growth factor is positive:

$$\sum_{r \in \mathcal{R}} \mathbb{S}_{sr}^- z_r \mathbf{x}_r \geq a_s, \quad \forall s \in \mathcal{M}, \quad (8)$$

ensuring that if a species is selected to be in  $\mathcal{M}$  ( $a_s = 1$ ), the contribution of this species must be non null in the growth factor.

- The species in  $\mathcal{M}$  must be autonomous ( $A^s$ ):

$$a_s \leq \left( \sum_{\substack{r \in \mathcal{R}: \\ \mathbb{S}_{sr}^+ > 0}} z_r \right) \left( \sum_{\substack{r \in \mathcal{R}: \\ \mathbb{S}_{sr}^- > 0}} z_r \right), \quad \forall s \in \mathcal{S}. \quad (9)$$

The conditions ensure that species in  $\mathcal{M}$  are selected only if they appear as both reactants and products in the chosen reactions. These constraints do not need to be explicitly incorporated into our model, as they are inherently satisfied by the finiteness of the growth factor.

- The reactions in the subnetwork must be autonomous ( $A^r$ ):

$$z_r \leq \left( \sum_{\substack{s \in \mathcal{S}: \\ \mathbb{S}_{sr}^+ > 0}} a_s \right) \left( \sum_{\substack{s \in \mathcal{S}: \\ \mathbb{S}_{sr}^- > 0}} a_s \right), \quad \forall r \in \mathcal{R}. \quad (10)$$

These constraints avoid activating reactions in case there are not autocatalytic species consumed and produced in the reactions.

These nonlinear constraints can be rewritten as linear constraints as follows:

$$\begin{aligned} \sum_{\substack{s \in \mathcal{S}: \\ \mathbb{S}_{sr}^+ \geq 1}} a_s &\geq z_r, & \forall r \in \mathcal{R}, \\ \sum_{\substack{s \in \mathcal{S}: \\ \mathbb{S}_{sr}^- \geq 1}} a_s &\geq z_r, & \forall r \in \mathcal{R}. \end{aligned}$$

That is, a reaction cannot be activated ( $z_r = 0$ ) if there are no autocatalytic species consumed/produced by the reaction (left-hand sides in the equations).

- The constructed subnetwork consists of at least one reaction:

$$\sum_{r \in \mathcal{R}} z_r \geq 1. \quad (11)$$

This condition avoids the construction of empty subnetworks.

The mathematical optimization model that we propose for solving the problem is then:

$$\begin{aligned}
& \max \alpha \\
& \text{s.t. (6) – (11),} \\
& \quad \mathbf{x} \in \mathbb{R}_+^{\mathcal{R}}, \\
& \quad a \in \{0, 1\}^{\mathcal{S}}, \\
& \quad z \in \{0, 1\}^{\mathcal{R}}, \\
& \quad \alpha \geq 0.
\end{aligned}$$

As noted for problem (MGF), this optimization model is neither convex nor concave. Furthermore, it involves binary variables, increasing its computational complexity. Despite these challenges, we propose several techniques to solve the problem exactly and efficiently.

First, we develop acceleration strategies to reduce the number of variables and constraints in the model without compromising the optimality of the solution (Section D). Second, we introduce an iterative approach that computes the subnetwork in a finite number of steps, with guaranteed convergence to the optimal solution. The details of these algorithms are provided in Algorithm 3.

Observe that, in an autocatalytic subnetwork  $\mathcal{G}' = (\mathcal{S}', \mathcal{R}')$ , every species in the set  $\mathcal{S}'$  might not be autocatalytic. The species  $s \in \mathcal{S}' \setminus \mathcal{M}$  are classified into three types (see Gagrani et al., 2024, and Fig. 2):

**Food Species:** : If  $s$  is only consumed by the reactions in  $\mathcal{R}'$  but not produced, i.e.,  $\mathbb{S}_{sr}^+ = 0$  for all  $r \in \mathcal{R}'$ , and  $\mathbb{S}_{sr}^- > 0$  for some  $r \in \mathcal{R}'$ .

**Waste Species:** : If  $s$  is only produced by the reactions in  $\mathcal{R}'$  but not consumed, i.e.,  $\mathbb{S}_{sr}^- = 0$  for all  $r \in \mathcal{R}'$ , and  $\mathbb{S}_{sr}^+ > 0$  for some  $r \in \mathcal{R}'$ .

**Non-autocatalytic species:** : If  $s$  is both consumed and produced by the reactions in  $\mathcal{R}'$  but its net change is negative under the productive flow that increases the autocatalytic species, i.e., there exists  $r_1, r_2$  such that  $\mathbb{S}_{sr_1}^- > 0$  and  $\mathbb{S}_{sr_2}^+ > 0$ , but for the flow  $\mathbf{x}$  that guarantees the productivity of the subnetwork (see condition (P)), one has that  $\sum_{r \in \mathcal{R}'} \mathbb{S}_{sr} \mathbf{x}_r < 0$ .

Note that, with the definitions above, and given a flow  $\mathbf{x}$  which ensures  $\mathcal{G}'$  is productive in  $\mathcal{M}$ , food and non-autocatalytic species are negatively produced by  $\mathcal{G}'$ , that is, for  $s \in \mathcal{S}'$  food or non-autocatalytic,  $\sum_{r \in \mathcal{R}'} \mathbb{S}_{sr} \mathbf{x}_r < 0$ . Thus, we call these species *negatively produced species* by  $\mathbf{x}$  and denote them by  $\mathcal{S}^-$ . Analogously, the waste species will be denoted by  $\mathcal{S}^+ := \mathcal{S}' \setminus (\mathcal{M} \cup \mathcal{S}^-)$ , and, together with the autocatalytic species, these are *positively produced*. Thus  $\mathcal{S}' = \mathcal{M} \cup \mathcal{S}^- \cup \mathcal{S}^+$ .

The construction of maximal growth factor subnetworks is a valuable tool for identifying the reactions and species that are most self-replicating and therefore most productive in a dynamic environment. Additionally, it may be necessary to construct maximal growth factor subnetworks under specific conditions tailored to particular scenarios. In Appendix C, we present several interesting cases and explain how they can be explicitly incorporated into the mathematical optimization model

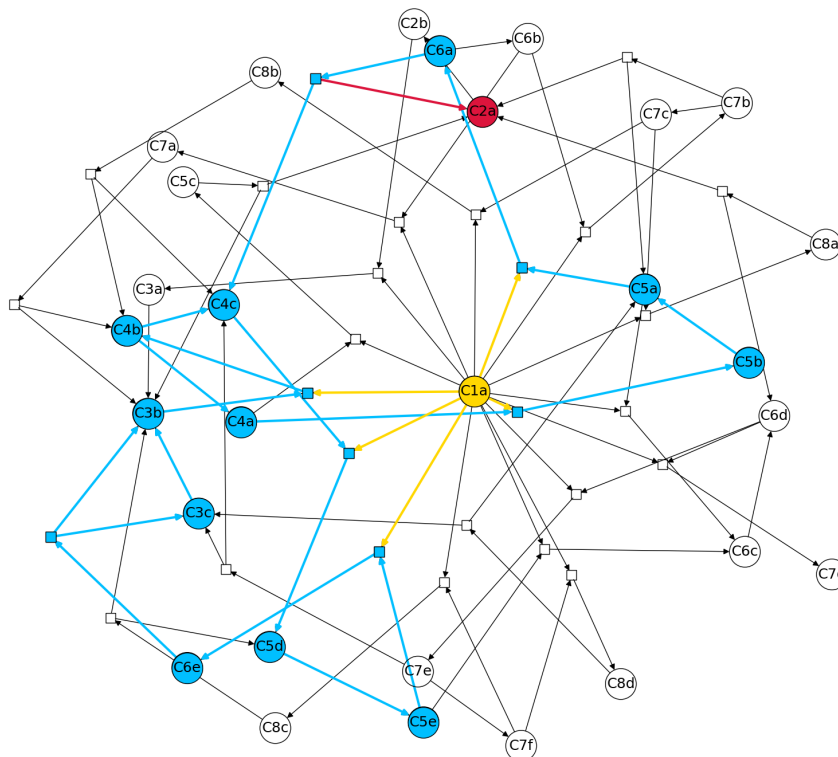


FIGURE 2. The Formose reaction network (Sec. 2) is shown and an autocatalytic subnetwork is highlighted. The food, waste, and autocatalytic species are shown in yellow, red, and blue, respectively. The reactions in the autocatalytic subnetwork can be found in Appendix F.1.

we propose for constructing maximal growth factor subnetworks. Specifically, we detail how to designate certain species or reactions as food, waste, or non-productive species within the resulting subnetwork using linear inequalities involving the decision variables already defined in our model.

**Economic implications of MGF.** Input-output analysis is a type of macroeconomic analysis that examines the interconnections between various economic sectors or industries (Christ, 1955). As shown in Table 1, under the mapping of species and reactions to goods and industries, respectively, CRNs can also be used to model an economy. In this framework, an economy is a network of industries, where each industry converts a multiset of input goods to a multiset of output goods (where the multiplicities can be fractional). The CRN framework of an economy is thus a natural framework for expressing interdependencies between industries and can be easily extended to incorporate elements such as human labor and scarce resources. In this remark, we describe how macroeconomists have traditionally applied the

CRN framework, albeit unknowingly, and how the framework developed here extends previous research.

In standard economic literature, macroeconomic input-output models are introduced with the pseudo-equation:

$$\begin{aligned} \text{Total amount produced} &= \\ \text{Internal demand} &+ \text{External demand,} \end{aligned}$$

for each good. In our formalism, this is formalized as,

$$\mathbb{S}^+ \mathbf{x} = \mathbb{S}^- \mathbf{x} + \mathbf{d}, \quad (12)$$

where  $\mathbf{d} \in \mathbb{R}_{\geq 0}^{\mathcal{S}}$  is the species demand vector,  $\mathbf{x} \in \mathcal{R}_{\geq 0}^{\mathcal{R}}$  is the operation intensity vector of industries, and  $\mathbb{S}^+$  and  $\mathbb{S}^-$  are respectively the output and input matrices modeling the economy.

To specialize to Leontief's input-output model (Leontief, 1986), one further assumes that each industry produces exactly one good while using any other combination of goods, and each good is produced by at least one industry. Under an appropriate normalization and choice of basis, this assumption yields that  $\mathbb{S}^+$  is the identity matrix  $\mathbb{I}$  and  $\mathbb{S}^-$  is a matrix  $\mathbb{A}$  that consists of only nonnegative off-diagonal entries. Substituting in (12) yields,

$$(\mathbb{I} - \mathbb{A}) \mathbf{x} = \mathbf{d}.$$

It can be shown that for any semi-positive vector  $\mathbf{d}$ , there exists a semi-positive solution  $\mathbf{x}$  to the above equation if the matrix  $(\mathbb{I} - \mathbb{A})$  is an M-matrix (Plemmons, 1977). The assumption that the stoichiometric matrix  $\mathbb{S} = \mathbb{S}^+ - \mathbb{S}^-$  is an M-matrix serves as the foundation for a substantial body of literature in mathematical economics.

The concept of a 'circularity' in economy can be formalized as an economy where each good (or a subset of goods) is produced and consumed by some industry, and each industry produces and consumes some good. The economy is 'growing' if it satisfies the productivity condition that there exist industry operation intensities that produce an excess of each good. Thus, the study of autocatalysis generalizes Leontief's input-output model to **growing circular** economies. As explained by Sargent and Stachurski (2024) and Gale (1989), the MGF is a solution to the generalized eigenvalue problem, and has been extensively studied in the context of M-matrices in the economics literature Li (2008). Moreover, the problem dual to Eq. MGF,

$$\begin{aligned} \beta(\mathcal{G}', \mathcal{M}) &:= \min \beta \\ \text{s.t.} \quad &\overline{\mathbb{S}^+}^T \mathbf{p} \leq \beta \overline{\mathbb{S}^-}^T \mathbf{p}, \\ &\overline{\mathbb{S}^+}^T \mathbf{p} \geq \mathbf{1}, \\ &\mathbf{p} \in \mathbb{R}_+^{\mathcal{R}'}, \beta \geq 0, \end{aligned}$$

is used to assign an optimal price vector to (autonomous) goods and  $\beta$  is interpreted as the optimal profit or interest factor. Perturbation inequalities concerning the compositionality of the growth and interest factors for M-matrices are derived in

Bapat et al. (1995). Deriving similar results for autocatalytic networks, which could inform the design of engineered economies or ecosystems, is left for future work.

**Role of MGF in dynamical systems.** For a CRN, an appropriate choice of kinetics on the reaction flows induces a dynamical system on the species concentration (or population) space. A popular choice of kinetics with widespread applications is *mass-action kinetics* (Yu and Craciun, 2018). Denoting the species concentration of species  $s$  as  $\nu_s$ , the reaction flow  $\mathbf{x}_r$  on a reaction  $r : r^- \rightarrow r^+$ , is given as

$$\mathbf{x}_r = k_r \nu^{r^-},$$

where  $r^-$  and  $r^+$  are, respectively, the input and output complex vectors  $\mathbb{S}_r^-$  and  $\mathbb{S}_r^+$ ,  $k_r$  is a positive scalar called the *rate-constant*, and the multi-index notation is employed

$$\nu^{r^-} := \prod_s \nu_s^{r_s^-}.$$

The dynamical system induced on the species concentrations under mass-action kinetics is given as,

$$\frac{d\nu_s}{dt} = \sum_r \mathbb{S}_s^r \mathbf{x}_r = \sum_r \mathbb{S}_s^r k_r \nu^{r^-}. \quad (13)$$

Let us denote the MGF for a CRN by  $\alpha$ . As shown in Lemma 2, if the CRN is autonomous (Def.1.1), then  $0 < \alpha < \infty$ . Furthermore, it can be shown that if the CRN is irreducible (von Neumann, 1945; Gale, 1989), there is a flow under which all the species attain the bound simultaneously for a reaction flow  $\mathbf{x}^*$ . At  $\mathbf{x}^*$  we get,

$$\mathbb{S}^+ \mathbf{x}^* = \alpha \mathbb{S}^- \mathbf{x}^*,$$

or equivalently, using the stoichiometric matrix  $\mathbb{S} = \mathbb{S}^+ - \mathbb{S}^-$ ,

$$\mathbb{S} \mathbf{x}^* = (\alpha - 1) \mathbb{S}^- \mathbf{x}^*. \quad (14)$$

An autonomous subnetwork is minimal if no species-reduced or reaction-reduced subnetwork is autonomous. Clearly, a minimal autonomous network is irreducible. Furthermore, for a minimal autonomous subnetwork, it can be shown that every reaction has a sole reactant, and every species is the sole reactant of exactly one reaction (see Lemma 3.2 in Gagrani et al. (2024), S.I. of Blokhuis et al. (2020)). This means that, by ordering the species in the order of the reactions of which they are the sole reactant, the input matrix  $\mathbb{S}^-$  for a minimal autonomous subnetwork is a diagonal matrix (see child-selection in Vassena and Stadler (2024)).

Substituting Eq.14 in Eq. 13 for a minimal autonomous network under the choice of basis discussed above, we get

$$\frac{d\nu_r}{dt} = (\alpha - 1) r^- k_r \nu_r^{r^-}, \quad (15)$$

where  $r^-$  is now a scalar. This is an equation of the form:

$$\frac{d\nu_r}{dt} = \kappa \nu_r^c,$$

where,

$$\kappa = (\alpha - 1)r^-k_r, \text{ and } c = r^-.$$

The above equation has solutions:

$$x(t) = \begin{cases} e^{\kappa t} \nu_r(0) & \text{for } c = 1 \\ (\nu_r(0)^{1-c} - (c-1)\kappa t)^{\frac{-1}{c-1}} & \text{for } c > 1, \end{cases}$$

where  $\nu(0)$  is the concentration at which the optimal flux is obtained, i.e.  $\mathbf{x}_r^* = k_r \nu_r(0)^{r^-}$ . Thus, the MGF is directly related to the exponential growth, decay, or finite time blowup that a dynamical system can exhibit.

## 2. RESULTS

The proposed methodologies have been empirically validated through two types of experiments. First, to validate the performance of the mathematical optimization models, we conducted computational experiments to stress-test the formulations and assess their dimensional limitations. These experiments also enable the comparison of the performance of the proposed algorithms on the same input data. Second, we apply our methodologies to two well-known real-world CRNs, namely the *Formose network* and *E. coli core metabolism*.

**Synthetic Experiments.** Appendix E presents a series of computational experiments designed to evaluate the performance of the three proposed algorithms across various synthetic instances. These instances are carefully generated using the Python software *SBbadger* proposed by Kochen et al. (2022) to reflect diverse problem characteristics, ensuring a thorough assessment of each algorithm’s efficiency, scalability, and robustness. The primary objective of these experiments is to validate the proposed method for computing the MGF of a given subnetwork. The results provide insights into the strengths and limitations of each algorithm and guide further optimization efforts.

As previously mentioned, detecting and enumerating autocatalytic subnetworks is a challenging (NP-complete) problem. However, the use of the Maximum Growth Factor (MGF) appears to mitigate the computational cost of these tasks, as illustrated in Figure 3. The left plot shows boxplots of the CPU times required to compute the subnetwork with the maximum MGF for synthetic instances with species counts ranging from 10 to 50 (x-axis). As observed, certifying the optimality of the subnetwork can, in the worst-case scenario, require hours of CPU time. In contrast, the right plot displays boxplots for the same instances, but focusing on the time required in the iterative procedure to find, for the first time, a subnetwork with an MGF greater than 1 (i.e., an autocatalytic subnetwork). In this case, the procedure took only a few seconds to identify an autocatalytic subnetwork.

The second interesting observation drawn from our experiments is that although the growth factor increases by the number of iterations of our algorithm, it stabilizes to a close-to-optimal growth factor in a few iterations, which means that one could find a good quality subnetwork (in terms of the MGF) in a few iterations. In Figure



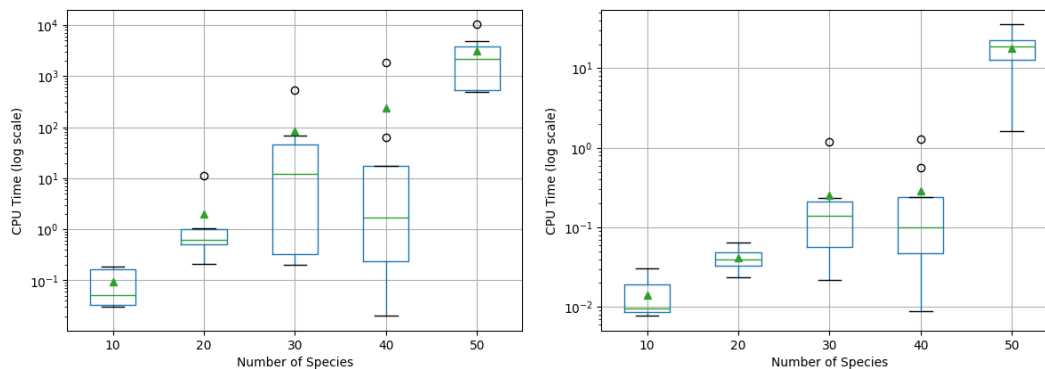


FIGURE 3. Boxplots of CPU times (in log scale) for two tasks across synthetic instances with 10 to 50 species. Time to compute the subnetwork with maximum MGF, which can take hours for larger instances (left). Time to first find an autocatalytic subnetwork (MGF  $> 1$ ), typically just a few seconds (right).

4 we show the trend of these MGFs as the number of iterations increases across varying number of species in the CRN.

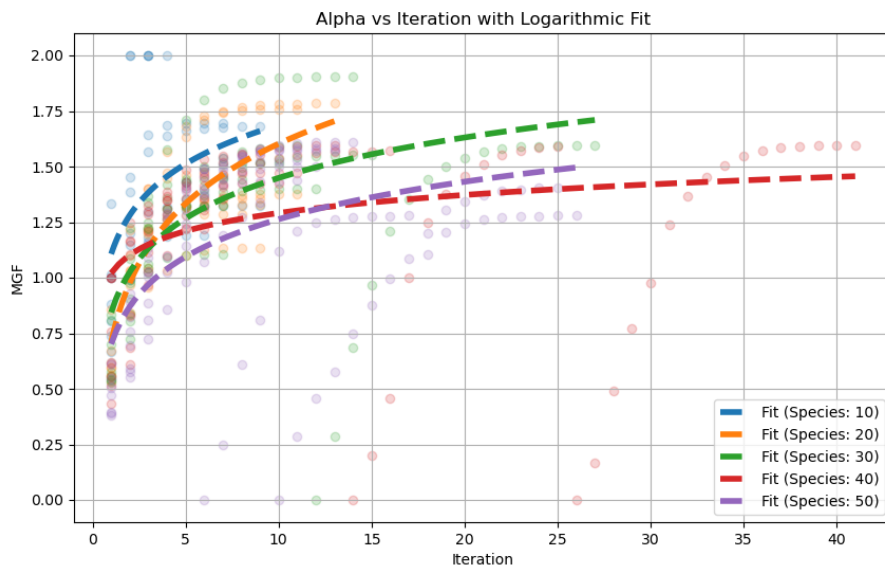


FIGURE 4. Evolution of the growth factor by the number of iterations of Algorithm 3.

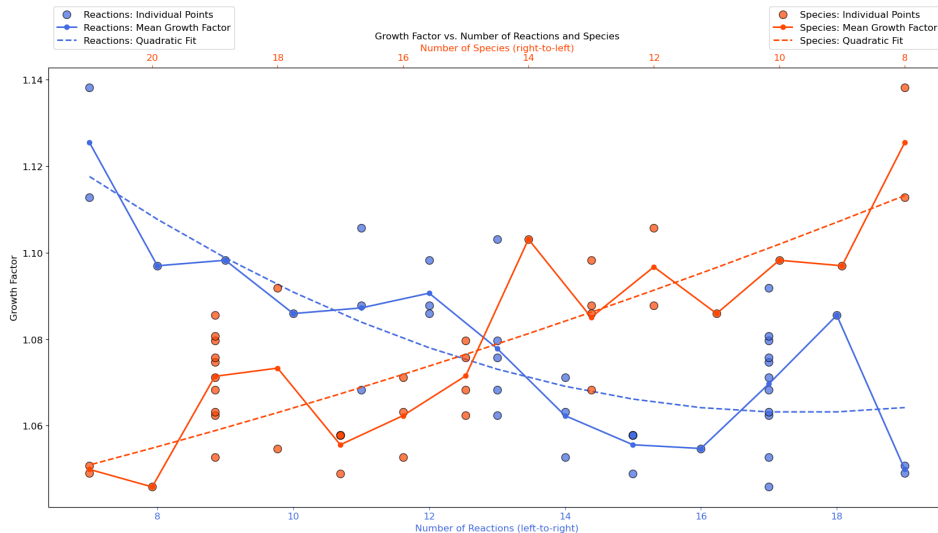


FIGURE 5. The dependence of the MGF on the shape of the autocatalytic cores (number of species and reactions) of the Formose network.

**Case Studies: Formose and E. coli.** We apply our methods to two well-known CRNs, namely the Formose reaction network and Escherichia (*E.*) coli metabolism. The Formose network finds application in prebiotic chemistry due to its ability to synthesize simple sugars including ribose—a precursor to DNA and RNA— from formaldehyde (C1a) (Benner et al., 2010). The *E. coli* metabolism has been extensively studied due to its well-characterized pathways, making it a model organism for understanding cellular processes, metabolic engineering, and synthetic biology applications (Palsson, 2015).

The functions of the algorithms used in our analysis are summarized as follows. Given an autonomous network, Algorithm 1 determines its MGF. For a given network, Algorithm 2 identifies the autonomous subnetwork with the maximum number of autonomous species. Finally, Algorithm 3 locates the autocatalytic subnetwork with the highest MGF within a given network. Henceforth, we refer to the autocatalytic core and the autocatalytic subnetwork with the highest MGF as the *strongest core* and the *strongest subnetwork*, respectively. For both case studies, we summarize the MGFs of their autocatalytic cores, discuss properties of the maximally autonomous network, and identify the strongest subnetworks.

*Formose reaction network.* The Formose network used in our study consists of 29 species and 38 reactions, and was taken from the Supplementary Material of Müller et al. (2022). We first used the algorithm for exhaustively enumerating all autocatalytic cores from Gagrani et al. (2024) and found 38 cores. We then used Algorithm 1 on them to identify their MGFs. In Figure 6 we show the distribution (histogram) of the growth factors for the whole set of cores of this CRN. The main observation

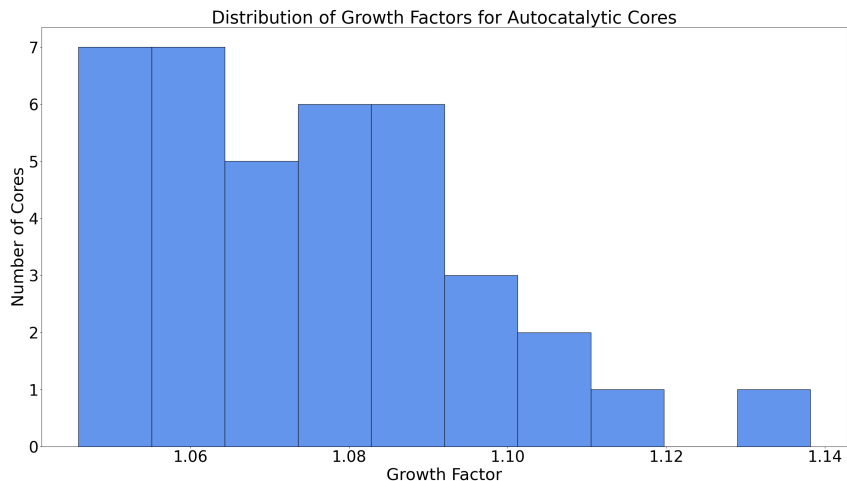


FIGURE 6. Histogram of the MGFs of the 38 autocatalytic cores found in the Formose reaction network.

from this distribution is that most of the cores have a *small* growth factor, whereas a few cores reach the maximum growth factor.

Next, we plot the top 3 cores with the highest MGF in Figure 7. Note that some of the reactions and species are shared by each of the three cores, for instance, species C4b and C3b appear in all of them.

Finally, Figure 5 illustrates the dependence of MGFs on the structure of the cores. As shown, cores with the highest MGFs contain the fewest reactions and species, while those with the lowest MGFs include the most. This observation supports the use of MGF as an alternative approach for constructing minimal autocatalytic subnetworks within a more flexible and informative framework.

In contrast to the previous case, where the algorithm for enumerating all autocatalytic cores from Gagrani et al. (2024) was employed, we now apply Algorithms 2 and 3 directly to the entire network. This approach leads to different conclusions:

**Alg. 2::** The algorithm completed in 2.09 seconds over 21 iterations, with an average iteration time of 0.01 seconds. All species except C1a (Formaldehyde) and C7d appear in the solution, resulting in a total of 27 autonomous species. Furthermore, the subnetwork is autocatalytic with an MGF of 1.13, demonstrating its ability to sustain and produce more of itself. The subnetwork where these species are autocatalytic, along with an optimal reaction flow assignment, is shown in the left panel of Figure 8.

Notably, to achieve the MGF, the majority of the flow is concentrated in the strongest autocatalytic core. This phenomenon was consistently observed across all instances where our algorithms were applied. Further investigation into this behavior is warranted, and we plan to explore it in future research.

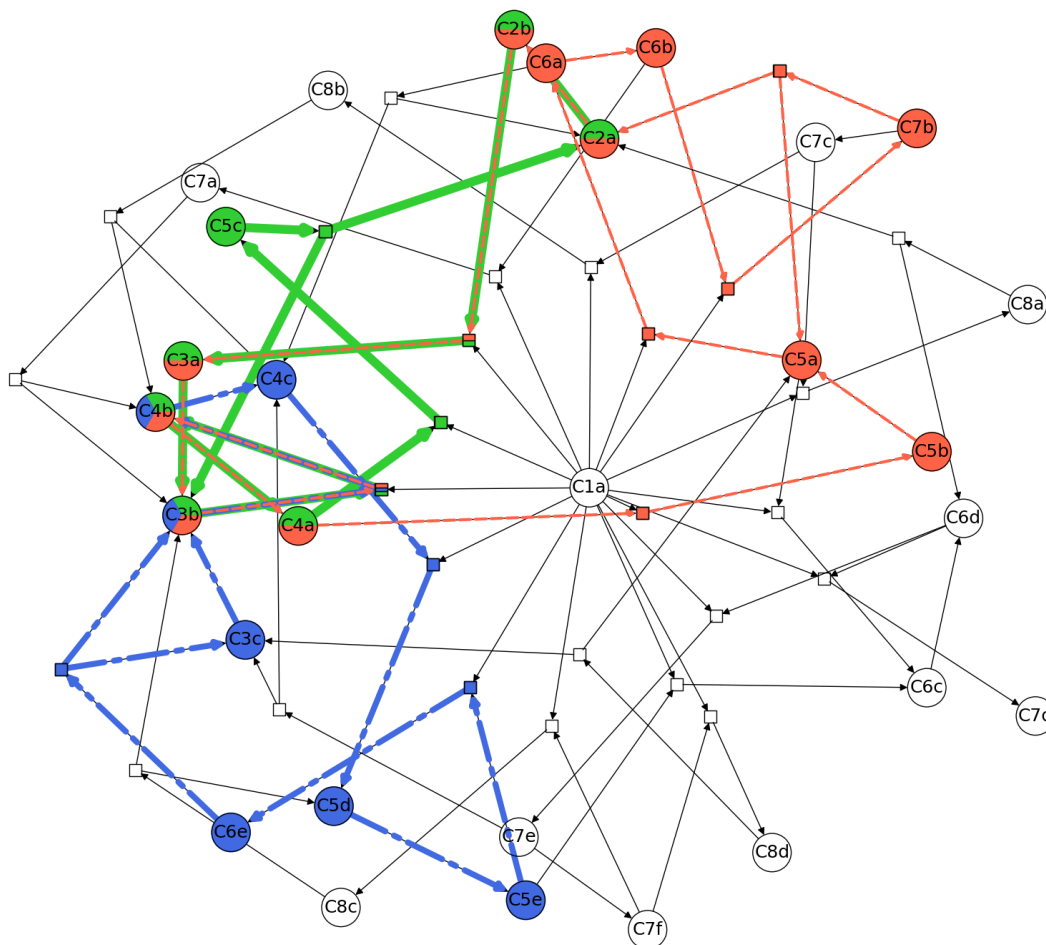


FIGURE 7. Autocatalytic cores with the top 3 MGFs for the *Formose* dataset, shown in green (MGF of 1.138), blue (1.112), and red (1.105). The details of the shown cores can be found in App. F.1.

**Alg. 3::** The algorithm completed in 1.6 seconds over 5 iterations, with an average iteration time of 0.32 seconds. The strongest subnetwork corresponds to the strongest core, with an MGF of 1.138, as shown independently in the right panel of Figure 8. It is also highlighted within the context of the entire network in the top panel of Figure 1.

As a core, it contains 7 autocatalytic species and 7 reactions. This indicates that, for the Formose network, any reactions outside the strongest core ultimately decrease the MGF of the network. This finding suggests that, at least for optimality, side reactions are detrimental to the network's autocatalytic growth.

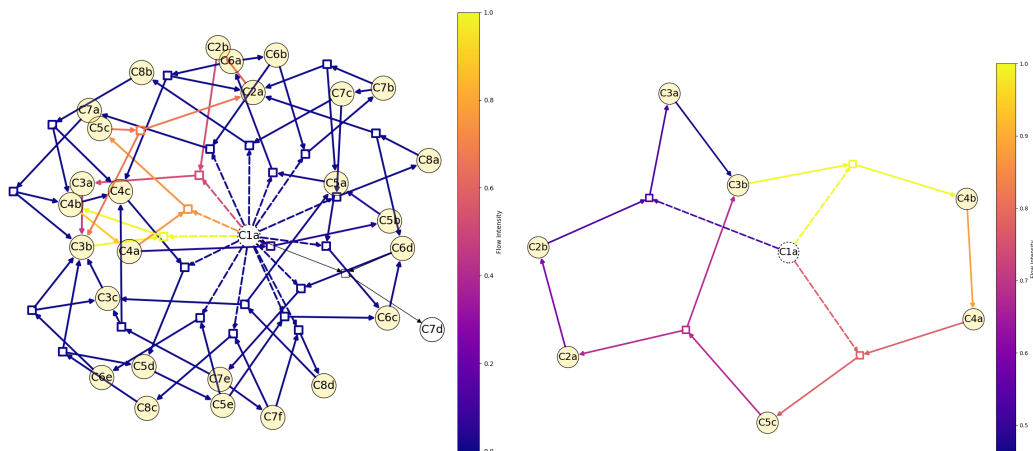


FIGURE 8. Application of Algorithms 2 and 3 on the Formose network. In the left panel, the autocatalytic subnetwork with the maximum number of autocatalytic species is shown. In the right panel, the autocatalytic subnetwork with the highest MGF (*strongest subnetwork*) is shown. For this network, the strongest subnetwork is the autocatalytic core with the highest MGF (also shown in green in the right panel of Figure 7).

Note that the solution provided by Algorithm 3 is always a subnetwork of the solution from Algorithm 2. This outcome is expected, as Algorithm 3, while selecting reactions, chooses a subset of the autocatalytic species identified by Algorithm 2.

*E. coli* metabolism. The *E. coli* core metabolism network used in our study consists of 72 species (metabolites) and 95 reactions. It was taken from the BiGG Models platform (King et al., 2016), a database of genome-scale metabolic network reconstructions, and the stoichiometric matrix was processed using the RULE-IT platform (Cuevas-Zuviria and Sokolskyi, 2024).

Similar to the approach in the previous case study, we enumerated all the autocatalytic cores in the network. We found a total of 581 cores and the histogram of their MGF distribution can be found in Figure 9. In this case, the conclusion obtained with the Formose dataset is even more evident, being in this case the number of cores with MGF slightly greater than one a vast majority of the cores.

The top three cores with the highest MGFs are shown in Figure 10. The species highlighted with white circles represent those required in the reactions—either as inputs (food), outputs (waste), or autonomous species that are non-autocatalytic. Observe that only a small subset of the reactions and species from the entire CRN are present in these maximal MGF networks.

Finally, the dependence of the MGFs on the shape of the core is shown in Figure 11. Similar to the previous case study, we see a clear trend of increase in the MGF for smaller cores with a lesser number of species and reactions.

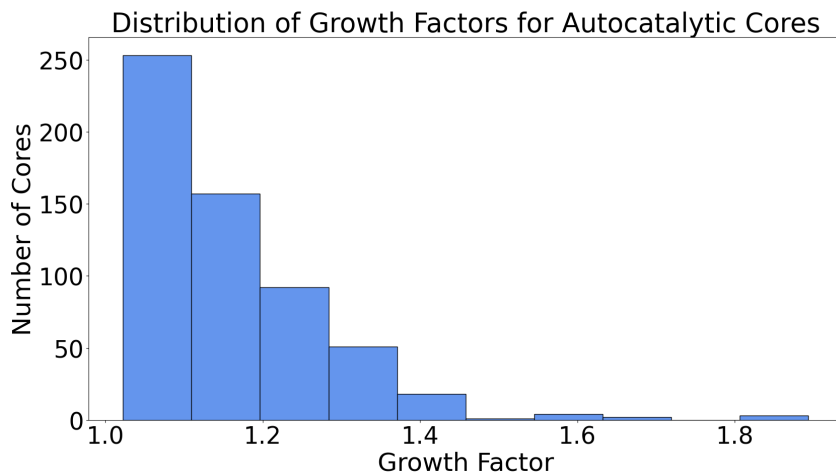


FIGURE 9. Histogram of the MGFs of the 581 autocatalytic cores found in the *E. coli* core metabolism.

**Alg. 2:** An application of Algorithm 2 reveals that the maximal autonomous subnetwork for the *E. coli* dataset comprises only 25 species. The algorithm completed in 1.55 seconds over 6 iterations, with an average iteration time of 0.26 seconds. The subnetwork, along with an optimal reaction flow assignment, is shown in Figure 12. Notably, the species *pi\_c*, which is autocatalytic in the three cores depicted in Figure 10, is not autonomous in this solution.

Unlike the Formose network, this subnetwork is not autocatalytic and has an MGF of 1. This indicates that, at best, the autonomous species can sustain themselves collectively at equilibrium. However, it is impossible for all autonomous species to simultaneously increase in concentration. Importantly, this conclusion is not a trivial consequence of mass conservation, as the subnetwork includes both a food and a waste set.

**Alg. 3:** Using Algorithm 3, the strongest subnetwork was identified and is presented in Fig. 1 and Fig. 13. The first figure depicts the solution within the context of the entire autonomous subnetwork, while the second highlights only the autocatalytic species and reactions involved.

The MGF of this subnetwork was found to be 2.77, significantly higher than that of the strongest core (MGF 1.89). The algorithm completed its execution in 234.58 seconds over 22 iterations, with an average iteration time of 10.66 seconds. The solution comprises 13 autocatalytic species and 13 reactions.

Interestingly, the largest autonomous subnetwork identified by Alg. 2 excludes one of the top-three cores with the highest MGF. Furthermore, all of the strongest cores are excluded in the strongest subnetwork identified by Alg. 3. This example highlights an important insight: several non-optimal cores can be combined, along with additional reactions not belonging to any core, to form a subnetwork with a higher MGF than any individual autocatalytic core within the network. The

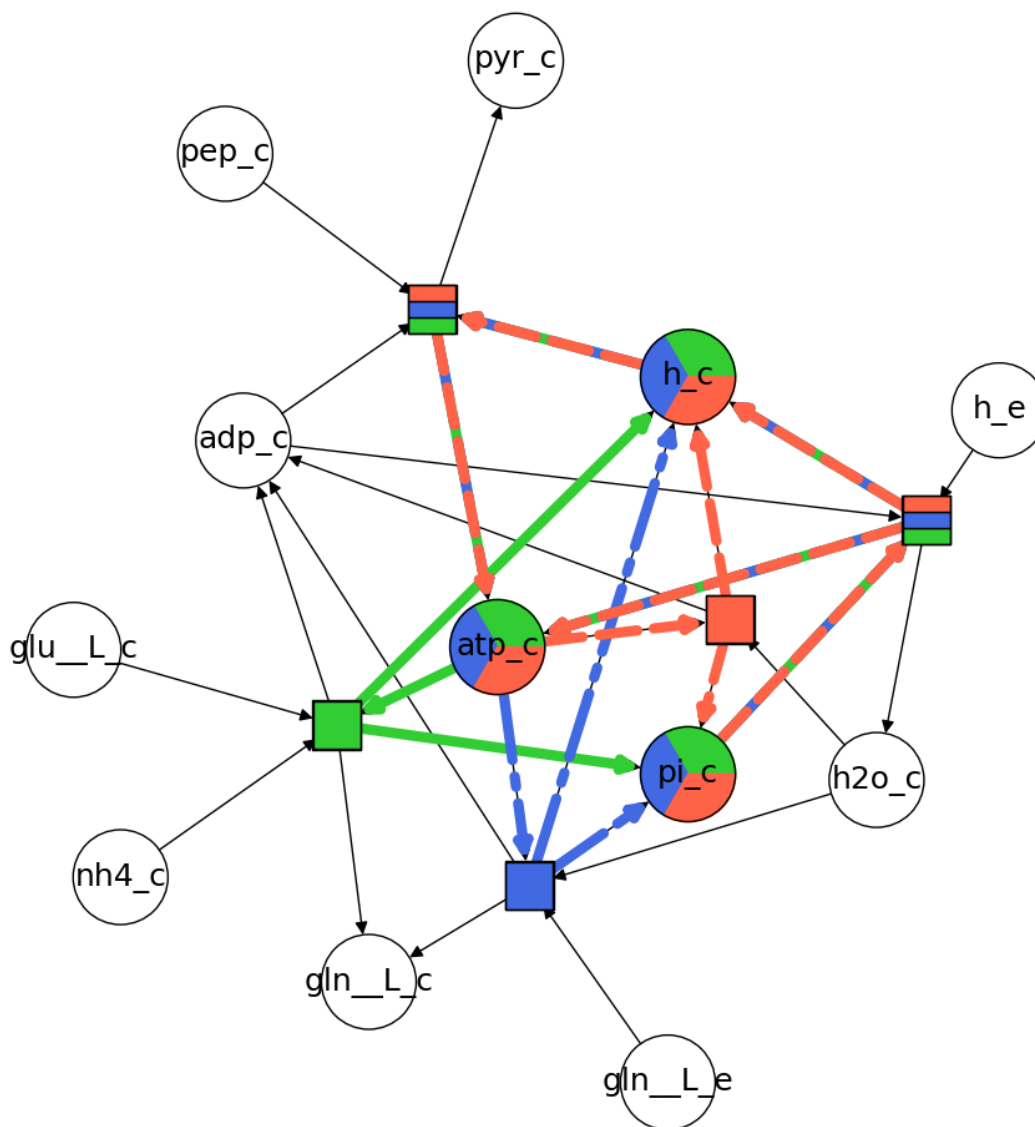


FIGURE 10. Autocatalytic cores with the highest MGFs. All 3 cores have a MGF of 1.89. The details of the shown cores can be found in App. F.2.

exploration of the biological implications of these results, as well as an investigation into whether this trend is consistent across other metabolic networks, is left for future research.

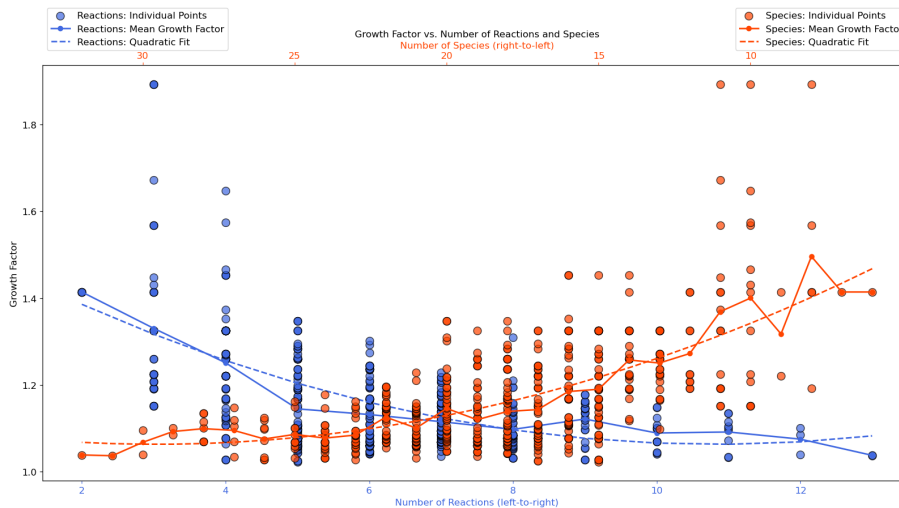


FIGURE 11. The dependence of the MGF on the shape of the autocatalytic cores (number of species and reactions) of the *E. coli* core metabolism.

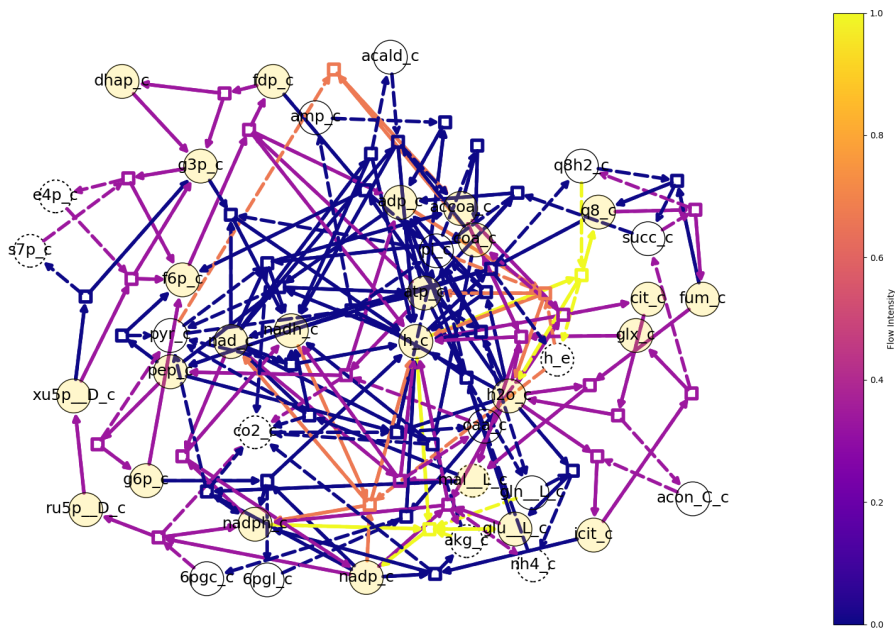


FIGURE 12. Application of Algorithms 2 on the *E. coli* metabolism. In the autocatalytic subnetwork with the maximum number of autocatalytic species is shown.



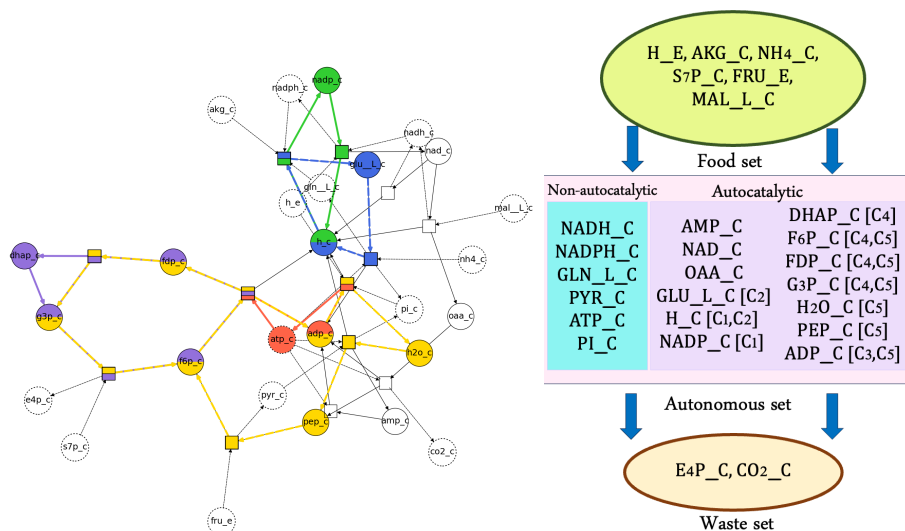


FIGURE 13. Application of Algorithm 3 on the *E. coli* metabolism. In the left panel, the strongest autocatalytic subnetwork is shown. The autocatalytic species are shown in solid circles, and every other species in the subnetwork is shown in dotted circles. The cores contained in the strongest subnetwork are also highlighted in different colors. In the right panel, the species decomposition of the species in the subnetwork into food, waste, non-autocatalytic, and autocatalytic sets is presented. We also indicate which core, if any, contains the autocatalytic species (Green-C1, Blue-C2, Orange-C3, Purple-C4, Yellow-C5). The reactions in the strongest subnetwork along with the reactions of autocatalytic cores contained inside of them can be found in App.F.2.

### 3. DISCUSSION

Topologically, CRNs are multi-directed hypergraphs that connect multisets of species (vertices) via reactions (directed hyperedges). The expressivity of CRNs and their widespread use in modeling stem from their ability to induce dynamics in species populations through the choice of kinetics governing the reaction flows (Yu and Craciun, 2018). These reaction flows are defined as specific functions of species concentrations and the reactions themselves. Popular choices include mass-action kinetics, Michaelis-Menten kinetics, and generalized mass-action kinetics, each with its own regime of validity and range of applications.

The ability to characterize the potential dynamics of a CRN solely based on its topology, independent of the choice of kinetics, greatly benefits both theoretical investigations and practical applications (Blanchini et al., 2014). The purpose of our framework is to extract such numerical values directly from the topology of a CRN. In the remainder of this section, we summarize the proposed metric, its

relationship to dynamics, the contributions of our work, and potential applications across disciplines.

The topology of CRN can be summarized a pair of matrices  $(\mathbb{S}^-, \mathbb{S}^+)$ , which we call the input-output matrices (Eq. 1). Taking inspiration from (von Neumann, 1945), we define a network’s Maximum Growth Factor (MGF) as (Def. 1.2)

$$\alpha = \sup_{\mathbf{x} \in \mathbb{R}_+^{\mathcal{R}}} \inf_{s \in \mathcal{S}} \frac{\sum_{r \in \mathcal{R}} \mathbb{S}_{sr}^+ \mathbf{x}_r}{\sum_{r \in \mathcal{R}} \mathbb{S}_{sr}^- \mathbf{x}_r}.$$

It is clear from the definition that it is a purely topological quantity and is invariant up to rescaling of the input and output vector of any reaction. Much like the relaxation speed of a chemical system is given by the speed of its slowest reaction (also called the ‘rate-limiting reaction’), the growth factor of a network, quantified by the MGF, is given as the maximum ratio of production to consumption of the slowest growing species in the network.

A MGF of  $\alpha = 0$ ,  $0 < \alpha < 1$ ,  $\alpha = 1$ ,  $1 < \alpha < \infty$ , and  $\alpha = \infty$  means that the network has no ability to produce, can consume more than it produces, can remain at equilibrium, can produce more than it consumes, and can produce indefinitely, respectively. If the CRN is autonomous in  $\mathcal{S}$  (1.1), then  $0 < \alpha < \infty$  (Lemma 2). Furthermore, in Thm. 1, we show that an autonomous network with  $\alpha > 1$  is an autocatalytic network. While our investigations focus on autocatalytic networks, our framework readily generalizes to *autoinhibitory networks*, i.e., autonomous networks with  $0 < \alpha < 1$ . It was recently shown in (Vassena and Stadler, 2024) that minimal autocatalytic subnetworks, referred to as (autocatalytic) cores, are unstable positive-feedbacks. By the same argument, minimal autoinhibitory networks can be shown to be negative-feedbacks.

In this work, we propose three novel mathematical optimization-based algorithms to calculate the MGF under different situations. Algorithm 1 computes the MGF for a given subnetwork of a CRN and in case the set of self-replicating species is given. The detection of the set of species, maximizing the MGF, when it is not provided, but still the subnetwork is given is performed by Algorithm 2. Finally, Algorithm 3 computes a subnetwork of a given CRN that maximizes the MGF, both detecting the self-replicating species and the reactions. Computing the MGF of a given autonomous subnetwork is an *easy* task (Algorithm 1), whereas detecting whether it is a core is NP-complete (Andersen et al.). Furthermore, although the construction of the MGF subnetwork can be computationally costly, the procedure can be stopped in case a MGF greater than one is detected, which is, in practice, found in the first iterations of Algorithm 3.

We applied our methods to two well-studied CRNs: the Formose reaction network (29 species, 38 reactions) and the E. coli core metabolism reaction network (72 species, 95 reactions). The Formose network is significant from an origins-of-life perspective because it generates longer molecules (up to 7 carbons) using a single-carbon molecule (formaldehyde) as a food source. In contrast, the E. coli

reaction network is extensively studied to understand cellular processes and develop applications in metabolic engineering.

For the Formose network, we found that the strongest autocatalytic subnetwork—i.e., the autocatalytic subnetwork with the highest MGF—was simply the strongest autocatalytic core. This suggests that any side reactions outside the autocatalytic core only serve to reduce the optimal growth rate achievable by the system. In contrast, for the *E. coli* metabolism, we found that the strongest autocatalytic subnetwork comprised five autocatalytic cores. Interestingly, none of these autocatalytic cores exhibited a significantly high MGF when considered in isolation, and the strongest autocatalytic cores were absent from the strongest autocatalytic subnetwork. This finding indicates a profound connection between autocatalysis and the role of natural selection in shaping metabolic pathways, a detailed analysis of which is left for future work.

Complex systems exhibit structure at multiple scales as species assemble into higher levels of organization, such as goods forming an economy, biomolecules constituting an organism, and organisms comprising an ecosystem. When modeled as a CRN, our framework assists in detecting and ranking subclasses of positive- and negative-feedbacks in the network. The role of feedbacks in complex systems—for maintaining homeostasis or exerting control—has been widely studied and cannot be overstated (Jones, 2012). In particular, when a specific outcome is desired, our framework can guide which new interactions need to be introduced and predict how the growth factor will change as a result. It is particularly useful in scenarios where new interactions can be introduced in a controlled manner, such as introducing organisms into an ecosystem or industries into an economy. To ensure that the maximum growth factor is achieved, the sequential expansion of the system can be performed gradually, allowing the system to equilibrate to its optimal growth factor after each addition. Although these applications for ecosystem engineering have not yet been fully developed, we hope that the unifying framework presented in this work will help pave the way forward.

#### ACKNOWLEDGEMENTS

Bruno Cuevas-Zuviría for providing the stoichiometric matrix of *E. coli* metabolism network and David Lacoste for useful comments.

#### FUNDING

VB and GG were partially supported by grant PID2020-114594GB-C21 funded by MICIU/AEI/10.13039/501100011033; grant RED2022-134149-T funded by MICIU/AEI/10.13039/501100011033 (Thematic Network on Location Science and Related Problems); grant C-EXP-139-UGR23 funded by the Consejería de Universidad, Investigación e Innovación and by the ERDF Andalusia Program 2021-2027, grant AT 21\_00032, and the IMAG-María de Maeztu grant CEX2020-001105-M/AEI/10.13039/501100011033. PG was partially funded by the National Science Foundation, Division of Environmental Biology (Grant No: DEB-2218817). PG was

partially funded by the National Science Foundation, Division of Environmental Biology (Grant No: DEB-2218817).

## REFERENCES

- Jakob L. Andersen, Christoph Flamm, Daniel Merkle, and Peter F. Stadler. Chemical transformation motifs—modelling pathways as integer hyperflows. 16(2):510–523. ISSN 1545-5963, 1557-9964, 2374-0043. doi: 10.1109/TCBB.2017.2781724. URL <https://ieeexplore.ieee.org/document/8171738/>.
- Jakob L Andersen, Christoph Flamm, Daniel Merkle, and Peter F Stadler. Maximizing output and recognizing autocatalysis in chemical reaction networks is np-complete. *Journal of Systems Chemistry*, 3(1):1–9, 2012.
- Jakob L Andersen, Christoph Flamm, Daniel Merkle, and Peter F Stadler. Defining autocatalysis in chemical reaction networks. *arXiv preprint arXiv:2107.03086*, 2021.
- Florin Avram, Rim Adenane, and Mircea Neagu. Advancing mathematical epidemiology and chemical reaction network theory via synergies between them. *Entropy*, 26(11):936, 2024.
- John C Baez and Blake S Pollard. A compositional framework for reaction networks. *Reviews in Mathematical Physics*, 29(09):1750028, 2017.
- Richard J Bagley, J Doyne Farmer, and Walter Fontana. Evolution of a metabolism. *Artificial life II*, 10:141–158, 1992.
- V Balakrishnan. *Network optimization*. Chapman and Hall/CRC, London, 2019.
- Julio R Banga. Optimization in computational systems biology. *BMC systems biology*, 2:1–7, 2008.
- RB Bapat, DD Olesky, and P Van Den Driessche. Perron-frobenius theory for a generalized eigenproblem. *Linear and Multilinear Algebra*, 40(2):141–152, 1995.
- Ana Isabel Barros, JBG Frenk, Siegfried Schaible, and Shuzhong Zhang. A new algorithm for generalized fractional programs. *Mathematical Programming*, 72:147–175, 1996.
- Stefano Benati, Justo Puerto, Antonio M Rodríguez-Chía, and Francisco Temprano. Overlapping communities detection through weighted graph community games. *Plos one*, 18(4):e0283857, 2023.
- Steven A Benner, Hyo-Joong Kim, Myung-Jung Kim, and Alonso Ricardo. Planetary organic chemistry and the origins of biomolecules. *Cold Spring Harbor perspectives in biology*, 2(7):a003467, 2010.
- Jean-Claude Bermond. *Hamiltonian graphs*, 1979.
- Franco Blanchini, Elisa Franco, and Giulia Giordano. A structural classification of candidate oscillatory and multistationary biochemical systems. *Bulletin of mathematical biology*, 76(10):2542–2569, 2014.
- Víctor Blanco, Safae ElHaj-BenAli, and Justo Puerto. Minimizing ordered weighted averaging of rational functions with applications to continuous location. *Computers & Operations Research*, 40(5):1448–1460, 2013.

- Alex Blokhuis, David Lacoste, and Philippe Nghe. Universal motifs and the diversity of autocatalytic systems. *Proceedings of the National Academy of Sciences*, 117(41):25230–25236, 2020.
- Carl F Christ. A review of input-output analysis. *Input-output analysis: An appraisal*, pages 137–182, 1955.
- Bruce L Clarke. Stoichiometric network analysis. *Cell biophysics*, 12:237–253, 1988.
- Jean-François Cordeau, Federico Pasin, and Marius M Solomon. An integrated model for logistics network design. *Annals of operations research*, 144:59–82, 2006.
- Jean-Pierre Crouzeix and Jacques A Ferland. Algorithms for generalized fractional programming. *Mathematical Programming*, 52:191–207, 1991.
- JP Crouzeix, JA Ferland, and S Schaible. An algorithm for generalized fractional programs. *Journal of Optimization Theory and Applications*, 47(1):35–49, 1985.
- Bruno Cuevas-Zuviria and Tymofii Sokolskyi. Rule-it: An online platform for reaction network explorations for chemical evolution. 2024.
- Armand Despons, Yannick De Decker, and David Lacoste. Structural constraints limit the regime of optimal flux in autocatalytic reaction networks. *Communications Physics*, 7(1):224, 2024.
- KA Dill and L Agozzino. Driving forces in the origins of life. *Open biology*, 11(2):200324, 2021.
- Martin Feinberg. Foundations of chemical reaction network theory. 2019.
- Jenna C Fromer and Connor W Coley. An algorithmic framework for synthetic cost-aware decision making in molecular design. *Nature Computational Science*, pages 1–11, 2024.
- Victor S Frost and Benjamin Melamed. Traffic modeling for telecommunications networks. *IEEE Communications Magazine*, 32(3):70–81, 1994.
- Praful Gagrani, Victor Blanco, Eric Smith, and David Baum. Polyhedral geometry and combinatorics of an autocatalytic ecosystem. *Journal of Mathematical Chemistry*, pages 1–67, 2024.
- David Gale. *The theory of linear economic models*. University of Chicago press, 1989.
- Ronald L Graham and Pavol Hell. On the history of the minimum spanning tree problem. *Annals of the History of Computing*, 7(1):43–57, 1985.
- Edward JS Hearnshaw and Mark MJ Wilson. A complex network approach to supply chain network theory. *International Journal of Operations & Production Management*, 33(4):442–469, 2013.
- Yuji Hirono, Takashi Okada, Hiroyasu Miyazaki, and Yoshimasa Hidaka. Structural reduction of chemical reaction networks based on topology. *Physical Review Research*, 3(4):043123, 2021.
- Frank K Hwang and Dana S Richards. Steiner tree problems. *Networks*, 22(1):55–89, 1992.
- Richard Jones. *Principles of biological regulation: an introduction to feedback systems*. Elsevier, 2012.

- Zachary A King, Justin Lu, Andreas Dräger, Philip Miller, Stephen Federowicz, Joshua A Lerman, Ali Ebrahim, Bernhard O Palsson, and Nathan E Lewis. Big models: A platform for integrating, standardizing and sharing genome-scale models. *Nucleic acids research*, 44(D1):D515–D522, 2016.
- Tetsuya J Kobayashi, Dimitri Loutchko, Atsushi Kamimura, Shuhei A Horiguchi, and Yuki Sughiyama. Information geometry of dynamics on graphs and hypergraphs. *Information Geometry*, pages 1–70, 2023.
- Michael A Kochen, H Steven Wiley, Song Feng, and Herbert M Sauro. Sbbadger: biochemical reaction networks with definable degree distributions. *Bioinformatics*, 38(22):5064–5072, 2022.
- Charles Kocher and Ken A Dill. Origins of life: first came evolutionary dynamics. *QRB discovery*, 4:e4, 2023.
- Thomas Kosc, Denis Kuperberg, Etienne Rajon, and Sylvain Charlat. Thermodynamic consistency of autocatalytic cycles. *bioRxiv*, pages 2024–10, 2024.
- Wassily Leontief. *Input-output economics*. Oxford University Press, 1986.
- Wu Li. A multi-agent growth model based on the von neumann-leontief framework. 2008.
- Stefan Müller, Christoph Flamm, and Peter F Stadler. What makes a reaction network “chemical”? *Journal of cheminformatics*, 14(1):63, 2022.
- Gita Naseri and Mattheos AG Koffas. Application of combinatorial optimization strategies in synthetic biology. *Nature communications*, 11(1):2446, 2020.
- Bernhard Palsson. *Systems biology*. Cambridge university press, 2015.
- Zhen Peng, Jeff Linderoth, and David A. Baum. The hierarchical organization of autocatalytic reaction networks and its relevance to the origin of life. *PLOS Computational Biology*, 18(9):e1010498. ISSN 1553-7358.
- Zhen Peng, Alex M Plum, Praful Gagrani, and David A Baum. An ecological framework for the analysis of prebiotic chemical reaction networks. *Journal of theoretical biology*, 507:110451, 2020.
- Zhen Peng, Klaus Paschek, and Joana C Xavier. What wilhelm ostwald meant by “autokatalyse” and its significance to origins-of-life research: Facilitating the search for chemical pathways underlying abiogenesis by reviving ostwald’s thought that reactants may also be autocatalysts. *BioEssays*, 44(9):2200098, 2022.
- Robert J Plemmons. M-matrix characterizations. i—nonsingular m-matrices. *Linear Algebra and its applications*, 18(2):175–188, 1977.
- Thomas J Sargent and John Stachurski. Intermediate Quantitative Economics with Python. [http://python.quantecon.org/\\_pdf/quantecon-python.pdf](http://python.quantecon.org/_pdf/quantecon-python.pdf), 2024. [Online].
- Alexander Schrijver. On the history of the shortest path problem. *Documenta Mathematica*, 17(1):155–167, 2012.
- Eric Smith and Harold J Morowitz. *The origin and nature of life on earth: the emergence of the fourth geosphere*. Cambridge University Press, 2016.
- Eörs Szathmáry. The origin of replicators and reproducers. *Philosophical Transactions of the Royal Society B: Biological Sciences*, 361(1474):1761–1776, 2006.

- Nicola Vassena and Peter F Stadler. Unstable cores are the source of instability in chemical reaction networks. *Proceedings of the Royal Society A*, 480(2285):20230694, 2024.
- Tomas Veloz, Pablo Razeto-Barry, Peter Dittrich, and Alejandro Fajardo. Reaction networks and evolutionary game theory. *Journal of mathematical biology*, 68:181–206, 2014.
- J von Neumann. A model of general economic equilibrium. *The Review of Economic Studies*, 13(1):1–9, 1945.
- Oliver Weller-Davies, Mike Steel, and Jotun Hein. Complexity results for autocatalytic network models. *Mathematical Biosciences*, 325:108365, 2020.
- Polly Y Yu and Gheorghe Craciun. Mathematical analysis of chemical reaction systems. *Israel Journal of Chemistry*, 58(6-7):733–741, 2018.

#### APPENDIX A. THEORETICAL RESULTS ON THE MAXIMUM GROWTH FACTOR

The following results allows to link the proposed maximum growth factor of a chemical subnetwork with the notion of autocatalytic subnetwork. These results are also crucial to prove Theorem 1 that stabilshes specifically this relationship.

**Lemma 2.** *If  $\mathcal{G}'$  is autonomous in  $\mathcal{M}$ , then  $0 < \alpha(\mathcal{G}', \mathcal{M}) < \infty$ .*

*Proof.* Autonomy of  $\mathcal{G}'$  in  $\mathcal{M}$  implies that every species is produced and every reaction consumes. Under these assumptions, Theorem 9.8 in Gale (1989) shows that a positive  $\alpha$  exists. The proof is based on the fact that each reaction consumes at least one species, ensuring that the denominator  $\sum_{r \in \mathcal{R}'} \mathbb{S}_{sr}^- \mathbf{x}_r > 0$  for any positive flow  $\mathbf{x}$ , implying  $\alpha(\mathcal{G}', \mathcal{M}) < \infty$ . Additionally, since each species is produced at least once, the numerator  $\sum_{r \in \mathcal{R}'} \mathbb{S}_{sr}^+ \mathbf{x}_r > 0$ , which guarantees that  $\alpha(\mathcal{G}', \mathcal{M}) > 0$ .  $\square$

**Lemma 3.** *The subnetwork  $\mathcal{G}'$  is productive in  $\mathcal{M}$  if and only if  $\alpha(\mathcal{G}', \mathcal{M}) > 1$ .*

*Proof.* The proof follows directly. If  $\mathcal{G}'$  is productive in  $\mathcal{M}$ , then there exists a flow  $\mathbf{x}$  such that  $\sum_{r \in \mathcal{R}'} \mathbb{S}_{sr}^+ \mathbf{x}_r > \sum_{r \in \mathcal{R}'} \mathbb{S}_{sr}^- \mathbf{x}_r$  for all  $s \in \mathcal{M}$ . Conversely, if  $\alpha > 1$ , this same relationship holds.  $\square$

**Lemma 4.** *If  $0 < \alpha(\mathcal{G}', \mathcal{M}) < \infty$ , then,  $\mathcal{G}'$  is species autonomous.*

*Proof.* Since  $\mathbb{S}^-$  is nonnegative, and for each  $s \in \mathcal{M}$  we have that  $\sum_{r \in \mathcal{R}'} \mathbb{S}_{sr}^+ \mathbf{x}_r > 0$  and  $\sum_{r \in \mathcal{R}'} \mathbb{S}_{sr}^- \mathbf{x}_r > 0$ , then there exists at least  $r, r' \in \mathcal{R}'$  with  $\mathbb{S}_{sr}^+ > 0$ ,  $\mathbb{S}_{sr'}^- > 0$  (species autonomous).

On the other hand, for all  $r \in \mathcal{R}'$  such that  $\mathbb{S}_{sr}^+ = 0$  for all  $s \in \mathcal{M}$ , because of the maximization criterion, the optimal value would be obtained always when  $x_r = 0$  for these reactions (which is equivalent to not consider them in the subnetwork).

Let  $Q = \{r \in \mathcal{R}' : \mathbb{S}_{sr}^- = 0, \forall s \in \mathcal{M}\}$ , then, the expression for the growth factor for a given  $x$  is:

$$\inf_{s \in \mathcal{M}} \frac{\sum_{r' \in \mathcal{R}'} \mathbb{S}_{sr'}^+ \mathbf{x}_{r'}}{\sum_{r \in \mathcal{R}'} \mathbb{S}_{sr}^- \mathbf{x}_r} = \inf_{s \in \mathcal{M}} \left( \frac{\sum_{r \in \mathcal{R}' \setminus \{Q\}} \mathbb{S}_{sr'}^+ \mathbf{x}_{r'}}{\sum_{r' \in \mathcal{R}' \setminus \{Q\}} \mathbb{S}_{sr'}^- \mathbf{x}_{r'}} + \frac{\sum_{r \in Q} \mathbb{S}_{sr}^+ \mathbf{x}_r}{\sum_{r' \in \mathcal{R}' \setminus \{Q\}} \mathbb{S}_{sr'}^- \mathbf{x}_{r'}} \right)$$

since the term  $\sum_{r \in Q} \mathbb{S}_{sr}^+ \mathbf{x}_r \geq 0$  only appears in the numerator of the expression, when maximizing in  $\mathbf{x}$ , the solution is reached for values  $x_r = \infty$  for  $r \in Q$ , and then  $\alpha(\mathcal{G}', \mathcal{M}) = \infty$ , contradicting the finiteness of the growth factor.  $\square$

In this appendix we also state the convergence result for the different algorithms:

**Theorem 5.** *If the feasible flow vectors  $\mathbf{x}$  are upper bounded, Algorithms 1, 2, and 3 converges linearly (in terms of the number of iterations) to their optimal solution.*

*Proof.* The proof follows by applying the results in Crouzeix et al. (1985) taking into account that the three MGF algorithms that we propose verify the hypotheses for their application. Specifically, it is not difficult to see that the feasible regions of the problems under study are compact and the functions involved in the quotients in the MGF are linear (so continuous).  $\square$



## APPENDIX B. PSEUDOCODES FOR THE PROPOSED ALGORITHMS

```

input :  $\mathcal{G}' = (\mathcal{S}', \mathcal{R}')$ ,  $\mathcal{M} \subset \mathcal{S}'$ ,  $it = 0$ , and  $\mathbf{x}_0 \in \mathbb{R}_+^{|\mathcal{R}'|}$ ,  $\overline{\mathbf{S}}^+ = \mathbb{S}_{|\mathcal{M}}^+$ ,  $\overline{\mathbf{S}}^- = \mathbb{S}_{|\mathcal{M}}^-$ 
output: The growth factor  $\alpha(\mathcal{G}', \mathcal{M})$ 
1 Stop=False
2 while Stop=False do
3   Define  $\alpha_{it}^t = \alpha(\mathbf{x}_{it})$  and solve the linear program:
      
$$(\rho, \bar{\mathbf{x}}_{it}) \in \arg \max \rho$$

      
$$\text{s.t. } \rho \leq \overline{\mathbf{S}}^+ \mathbf{x} - \alpha_{it} \overline{\mathbf{S}}^- \mathbf{x},$$

      
$$\overline{\mathbf{S}}^- \mathbf{x} \geq \mathbf{1},$$

      
$$\mathbf{x} \in \mathbb{R}_+^{|\mathcal{R}'|}, \rho \in \mathbb{R}_+.$$

      if  $\rho = 0$  then
4     Stop=True,
5      $\alpha(\mathcal{G}', \mathcal{M}) = \alpha_{it}$ 
6   else
7      $\mathbf{x}_{it+1} = \bar{\mathbf{x}}_{it}$ ,
8      $it = it + 1$ 
9   end
10 end

```

**Algorithm 1:** Computation of the growth factor of subnetwork  $\mathcal{G}'$  with given set of self-replicating species  $\mathcal{M}$ .

```

input :  $\mathcal{G}' = (\mathcal{S}', \mathcal{R}')$ ,  $\text{it} = 0$ , and  $\mathbf{x}_0 \in \mathbb{R}_+^{|\mathcal{R}'|}$ 
output:  $\mathcal{M} \subseteq \mathcal{S}'$  and  $\alpha(\mathcal{G}', \mathcal{M}) = \max_{\mathcal{M}' \subseteq \mathcal{S}'} \alpha(\mathcal{G}', \mathcal{M}')$ .
1 Stop=False
2 while Stop=False do
3   Compute  $\alpha_{\text{it}} = \alpha(\mathcal{G}', \mathcal{M}, \mathbf{x}_{\text{it}})$ .
4   Solve the following linear program:
       $(\rho, \bar{\mathbf{x}}_{\text{it}}) \in \arg \max \rho$ 
      s.t.  $\rho \leq \mathbb{S}^+ \mathbf{x} - \alpha_{\text{it}} \mathbb{S}^- \mathbf{x} + M(1 - a_s), \quad \forall s \in \mathcal{S}',$ 
            $\mathbb{S}^- \mathbf{x} \geq \mathbf{a}, \quad ,$ 
            $\sum_{s \in \mathcal{S} | \mathbb{S}_{sr}^+ \geq 1} a_s \geq 1, \quad \forall r \in \mathcal{R}',$ 
            $\sum_{s \in \mathcal{S} | \mathbb{S}_{sr}^- \geq 1} a_s \geq 1, \quad \forall r \in \mathcal{R}',$ 
            $a_s \in \{0, 1\}, \quad \forall s \in \mathcal{S}',$ 
            $\mathbf{x} \in \mathbb{R}_+^{|\mathcal{R}'|}, \rho \in \mathbb{R}_+.$ 
      if  $\rho = 0$  then
5     Stop=True,
6      $\mathcal{M} = \{s \in \mathcal{S}' : a_s = 1\},$ 
7      $\alpha(\mathcal{G}', \mathcal{M}) = \alpha_{\text{it}}$ 
8   else
9      $\mathbf{x}_{\text{it}+1} = \bar{\mathbf{x}}_{\text{it}},$ 
10     $\text{it} = \text{it} + 1$ 
11  end
12 end

```

**Algorithm 2:** Selection of the set of self-replicating species,  $\mathcal{M}$ , that Maximizes the Growth Factor of Subnetwork  $\mathcal{G}'$ .

```

input :  $\mathcal{G} = (\mathcal{S}, \mathcal{R})$ ,  $\text{it} = 0$ , and  $\mathbf{x}_0 \in \mathbb{R}_+^{|\mathcal{R}'|}$ 
output: A subnetwork  $\mathcal{G}' = (\mathcal{S}', \mathcal{R}') \subseteq \mathcal{G}$  autonomous on  $\mathcal{M}$  with maximal
        growth factor  $\alpha(\mathcal{G}', \mathcal{M})$ .
1 Stop=False
2 while Stop=False do
3   Define  $\alpha_{\text{it}}^t = \alpha(\mathbf{x}_{\text{it}})$  and solve the linear program:
         $(\rho, \bar{\mathbf{x}}_{\text{it}}) \in \arg \max \rho$ 
        s.t.  $\rho \leq (\mathbb{S}^+ \mathbf{x})_s a_s z - \alpha_{\text{it}} (\mathbb{S}^- \mathbf{x})_s a_s z, \quad \forall s \in \mathcal{M},$ 
         $\mathbf{x} \in \mathbb{R}_+^{|\mathcal{R}'|}, \rho \geq 0,$ 
         $(y, a, s) \in \mathcal{X}$ 
        if  $\rho = 0$  then
4     Stop=True,
5      $\mathcal{S}' = \{s \in \mathcal{S} : y_s = 1\},$ 
6      $\mathcal{R}' = \{r \in \mathcal{R} : z_r = 1\},$ 
7      $\mathcal{M} = \{s \in \mathcal{S} : a_s = 1\}$ , and
8      $\alpha(\mathcal{G}', \mathcal{M}) = \alpha_{\text{it}}$ 
9   else
10     $\mathbf{x}_{\text{it}+1} = \bar{\mathbf{x}}_{\text{it}}$ 
11     $\text{it} = \text{it} + 1$ 
12  end
13 end

```

**Algorithm 3:** Computation of the subnetwork  $\mathcal{G}'$  and the self-replicating species  $\mathcal{M}'$  maximizing the MGF if a given CRN.

where

$$\mathcal{X} = \left\{ (a, z) \in \{0, 1\}^{\mathcal{S}} \times \{0, 1\}^{\mathcal{R}} : (a, s) \text{ verifies (7) - (11)} \right\}$$

### APPENDIX C. INCORPORATING FEATURES TO THE MATHEMATICAL MODEL

The following conditions can be incorporated to our mathematical optimization model to derive *special* subnetworks. Those are based on using an additional set of binary variables to identify the species that are part of the subnetwork:

$$y_s = \begin{cases} 1 & \text{if } s \in \mathcal{S}', \\ 0 & \text{otherwise.} \end{cases}$$

This set of variables is adequately defined by the following set of inequalities:

$$y_s \geq z_r, \quad \forall s \in \mathcal{S} \text{ such that } \mathbb{S}_{sr}^+ + \mathbb{S}_{sr}^- > 0, \quad (16)$$

$$y_s \leq \sum_{r \in \mathcal{R}: \mathbb{S}_{sr}^+ + \mathbb{S}_{sr}^- > 0} z_r, \quad \forall s \in \mathcal{S}, \quad (17)$$

$$a_s \leq y_s, \quad \forall s \in \mathcal{S}. \quad (18)$$

That is, if reaction  $r$  is part of the subnetwork ( $z_r = 1$ ), then, all the species involved such a reaction (as reactant or product) must be *activated* to be part of the subnetwork; and if all the reactions in the CRN in which an species  $s$  is either reactant or product, are not used in the subnetwork, then, the species will not be used either in the subnetwork. The last set of constraints assures that the set of self-replicating species (those with  $a_s = 1$ ) are chosen from the whole set of activated species ( $y_s = 1$ ).

- **Subnetworks with specific food set:** Particular species can be considered as food species, which are assumed to be available in nature, and only consumed by the system but never produced. Let us assume that one desires to construct subnetworks with maximal growth factor among those that consume a fixed subset of food species,  $\mathcal{F} \subset \mathcal{S}$ . This condition can be imposed to our model with the following sets of constraints:

$$y_s = 1, \quad \forall s \in \mathcal{F}, \quad (19)$$

$$z_r = 0, \quad \forall r \in \mathcal{R} : \exists s \in \mathcal{F} \text{ with } \mathbb{S}_{sr}^+ > 0. \quad (20)$$

The first equations enforce that the food species are activated species in the subnetwork, whereas the second set of constraints avoid the production of the food species by the system.

- **Subnetworks with specific waste species:** Similarly to the previous consideration, some species are considered to be only produced but never consumed in the system. Let us assume that one desires to construct subnetworks with maximal growth factor among those that consume a fixed subset of waste species,  $\mathcal{W} \subset \mathcal{S}$ . This condition can be imposed to our model with the following sets of constraints:

$$y_s = 1, \quad \forall s \in \mathcal{W}, \quad (21)$$

$$z_r = 0, \quad \forall r \in \mathcal{R} : \exists s \in \mathcal{W} \text{ with } \mathbb{S}_{sr}^- > 0. \quad (22)$$

Analogously to the previous specifications, the first equations enforce that the waste species are activated species in the subnetwork, whereas the second set of constraints avoid the consumption of these species by the system.

- **Subnetworks with specific non-autocatalytic species:** In case a set of species  $\mathcal{N} \subset \mathcal{S}$  is assumed to be consumed and produced by the system, but with a negative net production, we can impose this condition by the following constraints:

$$y_s = 1, \quad \forall s \in \mathcal{N}, \quad (23)$$

$$z_r = 0, \quad \forall r \in \mathcal{R} : \exists s \in \mathcal{N} \text{ with } \mathbb{S}_{sr}^- \cdot \mathbb{S}_{sr}^+ = 0, \quad (24)$$

$$(\mathbb{S}_s^+ - \mathbb{S}_s^-)\mathbf{x} \leq 0, \quad \forall s \in \mathcal{N}. \quad (25)$$

The first equations enforce that the non-autocatalytic species are activated species in the subnetwork. The second set of constraints avoid only the consumption or production of these species in the system. Finally, to avoid

the consideration of these species as *autocatalytic* species, the net production of these species is enforced to be nonpositive.

All these constraints can be combined, that is, if  $(\mathcal{F}, \mathcal{W}, \mathcal{N})$  is a triplet of desired food, waste, and non-autocatalytic desired species, respectively, the above conditions can be imposed in our model as:

$$y_s = 1, \quad \forall s \in \mathcal{F} \cup \mathcal{W} \cup \mathcal{N}, \quad (26)$$

$$z_r = 0, \quad \forall r \in \mathcal{R} : \sum_{s \in \mathcal{F}} \mathbb{S}_{sr}^+ > 0, \quad (27)$$

$$z_r = 0, \quad \forall r \in \mathcal{R} : \sum_{s \in \mathcal{W}} \mathbb{S}_{sr}^- > 0, \quad (28)$$

$$z_r = 0, \quad \forall r \in \mathcal{R} : \exists s \in \mathcal{N} \text{ with } \mathbb{S}_{sr}^- \cdot \mathbb{S}_{sr}^+ = 0, \quad (29)$$

$$(\mathbb{S}_s^+ - \mathbb{S}_s^-)\mathbf{x} \leq 0, \quad \forall s \in \mathcal{N}. \quad (30)$$

## APPENDIX D. SPEED-UP STRATEGIES

**D.1. Reducing the set of potential species and reactions.** The complexity of the mathematical optimization that we propose to extract a subnetwork of a given CRN with maximum growth factor depends of the number of variables and constraints that it involves. Specifically, the time required to solve the problem is affected by the number of reactions and species in the CRN. In order to reduce the search, we propose a preprocessing procedure that consists of removing from the list of species and reactions in the CRN, those that will never participate in such a subnetwork.

This procedure is outlined in Algorithm 4, which iteratively removes non-autonomous rows and columns from the input matrix  $M_1$  and the output matrix  $M_2$ . Note that those species that do not appear as both consumed and produced by the reactions are not required in our search. Once these species are removed from the list, it may happen that some of the reactions only consume or produce but not both, and then, they can be also avoided in the list. This process can be iteratively applied until no reactions or species are removed.

The procedure begins by initializing all rows and columns for inspection (lines 1-3). It then enters a loop to iteratively detect and remove null rows and columns (lines 4-27). At each iteration, null rows are identified by checking if the sum of entries in a row is zero in both  $M_1$  and  $M_2$  (lines 7-11). Similarly, null columns are detected by examining the column sums in  $M_1$  and  $M_2$  (lines 12-16). If no new null rows or columns are found, the algorithm terminates (lines 17-19).

When null rows or columns are detected, they are removed from  $M_1$  and  $M_2$  (lines 20-27). The sets of rows and columns to inspect are updated accordingly, ensuring that any newly created null rows or columns are included in subsequent iterations. This process repeats until no further null rows or columns are found, at which point the simplified matrices are returned (line 28).

```

input :  $M_1, M_2$ 
output:  $M_1, M_2$ 
1  $M_1, M_2 \in \mathbb{N}^{m \times n}$ 
2  $rows\_to\_check = \{1, \dots, m\}$ 
3  $columns\_to\_check = \{1, \dots, n\}$ 
4 while True do
5    $new\_null\_rows = \{\}$ 
6    $new\_null\_columns = \{\}$ 
7   for  $i$  in  $rows\_to\_check$  do
8     if  $\sum_{i=1}^m (M_1)_{ij} < 0$  or  $\sum_{i=1}^m (M_2)_{ij} < 0$  then
9        $new\_null\_rows.insert(i)$ 
10    end
11  end
12  for  $j$  in  $columns\_to\_check$  do
13    if  $\sum_{j=1}^n (M_1)_{ij} < 0$  or  $\sum_{j=1}^n (M_2)_{ij} < 0$  then
14       $new\_null\_columns.insert(j)$ 
15    end
16  end
17  if  $new\_null\_rows = \emptyset$  and  $new\_null\_columns = \emptyset$  then
18    break
19  end
20  for  $row$  in  $new\_null\_rows$  do
21     $remove\ row\ from\ M_1$ 
22     $remove\ row\ from\ M_2$ 
23  end
24  for  $column$  in  $new\_null\_columns$  do
25     $remove\ column\ from\ M_1$ 
26     $remove\ column\ from\ M_2$ 
27  end
28   $M_1, M_2 \in \mathbb{N}^{m \times n}$ 
29   $rows\_to\_check = \{1, \dots, m\}$ 
30   $columns\_to\_check = \{1, \dots, n\}$ 
31 end
32 return  $M_1, M_2$ 

```

**Algorithm 4:** Algorithm that remove all non autonomous rows and Columns from the input and output matrix.

**D.2. Clustering of CRNs into Connected Components.** Note that in case the CRNs is not connected, the MGF can be calculated, separately, in each of its connected components, and the MGF will be the maximum of all of them.

**Theorem 6.** Let  $\mathcal{G}_1 = (\mathcal{S}_1, \mathcal{R}_1), \dots, \mathcal{G}_k = (\mathcal{S}_k, \mathcal{R}_k)$  the different connected components for a CRN  $\mathcal{G} = (\mathcal{S}, \mathcal{R})$ . Let  $\mathcal{G}' = (\mathcal{S}', \mathcal{R}')$  be the maximal growth factor

subnetwork for  $\mathcal{G}$ , with set of autocatalytic species  $\mathcal{M}$ . Then:

$$\alpha(\mathcal{G}) = \max_{l=1,\dots,k} \alpha(\mathcal{G}_l),$$

where  $\mathcal{M}_l$  is the optimal set of autocatalytic species for the subnetwork  $\mathcal{G}_l$ , for  $l = 1, \dots, k$ .

*Proof.* The proof follows by noting that for any set  $\mathcal{M} \subset \mathcal{S}'$  and any flow  $\mathbf{x} = (x^1, \dots, x^k)$ —the flow decomposed by connected components:

$$\alpha(\mathcal{G}', \mathcal{M}, \mathbf{x}) = \min_{s \in \mathcal{M}} \frac{\sum_{r \in \mathcal{R}'} \mathbb{S}_{sr}^+ \mathbf{x}_r}{\sum_{r \in \mathcal{R}'} \mathbb{S}_{sr}^- \mathbf{x}_r} = \min_{l=1,\dots,k} \min_{s_l \in \mathcal{M}_l} \frac{\sum_{r \in \mathcal{R}_l} \mathbb{S}_{s_l r}^+ \mathbf{x}_r}{\sum_{r \in \mathcal{R}_l} \mathbb{S}_{s_l r}^- \mathbf{x}_r} = \min_{l=1,\dots,k} \alpha(\mathcal{G}_l, \mathcal{M}_l, \mathbf{x}^l).$$

Thus,

$$\alpha(\mathcal{G}') = \max_{\substack{\mathcal{M} \subset \mathcal{S}' \\ \mathbf{x} \in \mathbb{R}_+^{\mathcal{R}'}}} \alpha(\mathcal{G}', \mathcal{M}, \mathbf{x}) = \max_{l=1,\dots,k} \max_{\substack{\mathcal{M}_l \subset \mathcal{S}_l \\ \mathbf{x}_l \in \mathbb{R}_+^{\mathcal{R}_l}}} \alpha(\mathcal{G}_l, \mathcal{M}_l, \mathbf{x}_l) = \max_{l=1,\dots,k} \alpha(\mathcal{G}_l).$$

□

Based on the above result, we propose a clustering approach to decompose the problem and then reduce the dimensions of each of the problems to be solved to obtain the maximum growth factor subnetwork.

This strategy is outlined in Algorithm 5, which identifies weakly connected components in a directed bipartite graph representing species and reactions. The graph is constructed from the input matrix  $M_1$  and the output matrix  $M_2$ , with the algorithm outputting submatrices for each connected component.

The graph is built by interpreting  $M_1$  and  $M_2$  as adjacency matrices. Nodes represent species and reactions, and directed edges are established as follows:

- A directed edge from a species node to a reaction node is added if the corresponding entry in  $M_1$  is positive.
- A directed edge from a reaction node to a species node is added if the corresponding entry in  $M_2$  is positive.

Once the graph is constructed, a traversal method is used to identify weakly connected components—subsets of nodes connected via paths, regardless of edge direction. Each component groups species and reactions that are directly or indirectly related.

For each weakly connected component, the algorithm determines the species and reactions it contains. It then extracts the corresponding submatrices from  $M_1$  and  $M_2$ , representing the interactions within the component. These submatrices, along with their associated species and reaction indices, form the output. The algorithm continues until all components are processed, returning a comprehensive list of submatrices for all components. This decomposition simplifies the analysis by breaking down complex networks into smaller, manageable subsystems.

```

input :  $M_1, M_2$ 
output:  $M_1, M_2$ 
1  $M_1, M_2 \in \mathbb{N}^{m \times n}$ 
2  $number\_of\_species = \{1, \dots, m\}$ 
3  $number\_of\_reactions = \{1, \dots, n\}$ 
4 for  $i \leftarrow 1$  to  $number\_of\_species$  do
5   for  $j \leftarrow 1$  to  $number\_of\_reactions$  do
6     if  $input\_matrix[i, j] > 0$  then
7       | Add edge  $(i, j)$  in  $G$ 
8     end
9     if  $output\_matrix[i, j] > 0$  then
10      | Add edge  $(j, i)$  in  $G$ 
11     end
12   end
13 end
14  $components \leftarrow$  List of weakly connected components of  $G$ 
15  $components\_all \leftarrow$  empty list
16 for  $component$  in  $components$  do
17    $species\_indices \leftarrow$  empty list
18    $reaction\_indices \leftarrow$  empty list
19   for  $node$  in  $component$  do
20     if  $node$  is Species then
21       | Append node to  $species\_indices$ 
22     end
23     else if  $node$  in Reaction then
24       | Append node to  $reaction\_indices$ 
25     end
26   end
27    $input\_submatrix \leftarrow$ 
28      $input\_matrix[species\_indices, reaction\_indices]$ 
29    $output\_submatrix \leftarrow$ 
30      $output\_matrix[species\_indices, reaction\_indices]$ 
31   Append  $(input\_submatrix, output\_submatrix)$  to  $components\_all$ 
32 end
33 return  $components\_all$ 

```

**Algorithm 5:** Algorithm to find weakly connected components and generate corresponding submatrices.

## APPENDIX E. COMPUTATIONAL EXPERIMENTS

**E.1. Instance Generation.** We generated a set of instances simulating different types of CRNs using the python library `SBbadger` publicly available at Kochen et al. (2022). We generate CRNs with different sizes as follows: For each  $n \in$



$\{10, 20, 30, 40, 50\}$  we randomly simulate 8 CRN with  $|\mathcal{S}| = n$ , using the function `generate_serial.models`. The software provides for us the stoichiometric matrices  $\mathbb{S}^+$  and  $\mathbb{S}^-$  required to compute the MGF with the different methodologies. The generated files are available at the Github repository [github.com/vblancoOR/mgf\\_autocatalysis](https://github.com/vblancoOR/mgf_autocatalysis).

**E.2. Detailed results for the computational experiments.** We applied Algorithm 1 to all the generated instances, using Gurobi 11.03 as the optimization solver on an Ubuntu 22.04.03 environment, with an AMD EPYC 7042p 24-Core Processor and 64 GB RAM. The maximum number of iterations for the algorithm was set to 1000.

For each instance, we recorded the following metrics for Algorithms 1, 2, and 3: the growth factor obtained at each iteration until convergence, the CPU time required for each iteration, and the corresponding feasible flow vector ( $\mathbf{x}$ ) achieving the growth factor. For Algorithm 2, we also recorded the set of autocatalytic species identified. Additionally, for Algorithm 3, we documented the species and reactions comprising the optimal subnetwork.

The detailed results obtained for the synthetic instances are available in the Github repository [github.com/vblancoOR/mgf\\_autocatalysis](https://github.com/vblancoOR/mgf_autocatalysis).

Table 2 presents the averaged results of the experiments. For each number of species in the CRN (first column) and each algorithm (second column), the table shows the average number of iterations and CPU time (in seconds)—listed in columns `it` and `Time`, respectively—required to reach the optimal MGF. It also displays the average number of iterations and CPU time needed to identify the first autocatalytic subnetwork, shown in columns `First_it` and `Time_First`.

As observed, the computational demands increase as the number of decisions required by the algorithms grows. As expected, identifying the optimal subnetwork is more challenging and time-consuming than other approaches. Nevertheless, while obtaining the optimal solution may be computationally expensive, detecting an autocatalytic subnetwork (and determining whether one exists) can be achieved within reasonable CPU times.

The following plots provide a visual representation of the algorithms’ performance, offering a more detailed illustration of the conclusions drawn from the experiments. In Figure 14, we show the average growth factor values obtained at each iteration for all the algorithms. Note that the  $\alpha$ -value of one is achieved within just a few iterations, while guaranteeing the optimality of the MGF requires additional iterations.

In Figure 15, we present the average CPU time required for each tested number of species. This information is further summarized in Figure 16, where the performance of all algorithms is plotted in the same figure, using a log scale for CPU time to facilitate interpretation. While Algorithms 1 and 2 require comparable computation times, Algorithm 3 is significantly more demanding in terms of time.

No. Species	Alg.	it	First_it	Time (secs.)	Time_First (secs.)
10	1	10.3	2.8	0.0882	0.0203
	2	11.2	2.5	0.0972	0.0206
	3	3.9	2.3	0.0921	0.0375
20	1	11.1	4.7	0.4811	0.1416
	2	11.0	4.7	0.5035	0.1169
	3	5.5	2.5	1.9684	0.0857
30	1	13.9	5.0	1.5921	0.2945
	2	13.2	4.5	1.6346	0.2965
	3	8.3	4.2	81.8758	24.7882
40	1	10.0	3.5	1.1954	0.3067
	2	10.2	3.0	1.4295	0.2725
	3	7.9	4.7	139.1985	114.9406
50	1	15.1	5.4	13.7698	2.6652
	2	13.8	5.1	15.3927	3.3996
	3	8.2	5.1	2566.3931	121.2335

TABLE 2. Average results of the synthetic experiments.

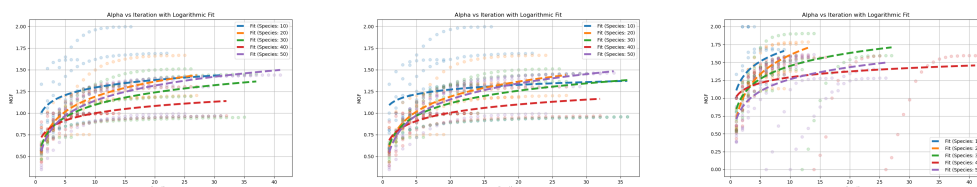


FIGURE 14. Growth factor values at each iteration for Algorithm 1 (left), Algorithm 2 (center), and Algorithm 3 (right).

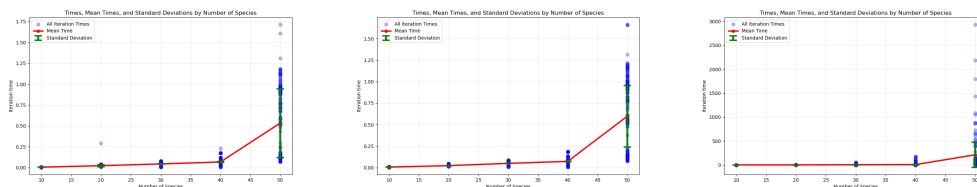


FIGURE 15. Variation in iteration time with the number of species for Algorithm 1 (left), Algorithm 2 (center), and Algorithm 3 (right).

## APPENDIX F. DETAILED RESULTS FOR THE CASE STUDIES

F.1. **Formose.** The details of the reaction subnetworks in different figures are shown. The reaction numbers are identical to those in the dataset.

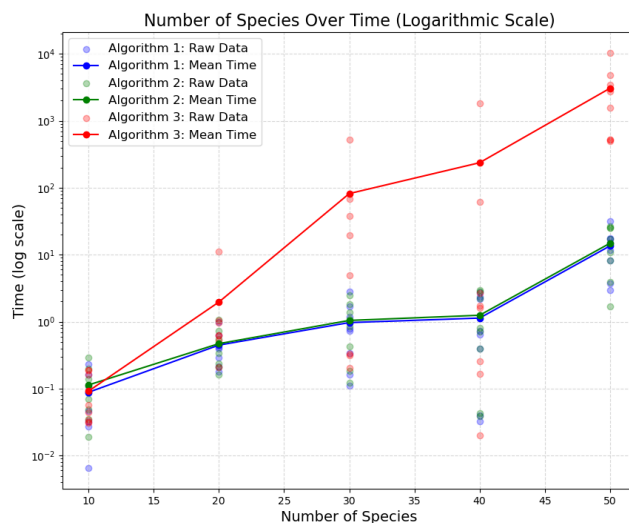


FIGURE 16. Total CPU time required by Algorithms 1, 2, and 3 to solve the instances, plotted for comparison.

TABLE 3. Summary of the information expressed in Fig. 2.

Category	Details
<b>Food Set</b>	{C1a formaldehyde}
<b>Waste Set</b>	{C2a}
<b>Autocatalytic Set</b>	{C3b, C3c dihydroxy acetone, C4b, C4c, C5a, C5d, C5e, C6a, C6c, C6d, C7e, C7f, C8d}
<b>Growth Factor</b>	1.0682640255462035
<b>Reactions</b>	
R4	C3c dihydroxy acetone $\rightarrow$ C3b
R5	C1a formaldehyde + C3b $\rightarrow$ C4b
R7	C4b $\rightarrow$ C4c
R10	C1a formaldehyde + C4c $\rightarrow$ C5d
R12	C5d $\rightarrow$ C5e
R13	C1a formaldehyde + C5a $\rightarrow$ C6a
R15	C1a formaldehyde + C5e $\rightarrow$ C6c
R18	C6c $\rightarrow$ C6d
R22	C1a formaldehyde + C6d $\rightarrow$ C7e
R24	C7e $\rightarrow$ C7f
R28	C1a formaldehyde + C7f $\rightarrow$ C8d
R32	C8d $\rightarrow$ C3c dihydroxy acetone + C5a
R36	C6a $\rightarrow$ C2a + C4c

TABLE 4. Summary of the green core from Fig. 7.

Category	Details
<b>Food Set</b>	{C1a formaldehyde}
<b>Autocatalytic Set</b>	{C2a, C2b, C3a, C3b, C4a, C4b, C5c}
<b>Growth Factor</b>	1.138163596847235
<b>Reactions</b>	
R1	C2a $\rightarrow$ C2b
R2	C1a formaldehyde + C2b $\rightarrow$ C3a
R3	C3a $\rightarrow$ C3b
R5	C1a formaldehyde + C3b $\rightarrow$ C4b
R6	C4b $\rightarrow$ C4a
R9	C1a formaldehyde + C4a $\rightarrow$ C5c
R38	C5c $\rightarrow$ C2a + C3b

TABLE 5. Summary of the blue core from Fig. 7.

Category	Details
<b>Food Set</b>	{C1a formaldehyde}
<b>Autocatalytic Set</b>	{C3b, C3c dihydroxy acetone, C4b, C4c, C5d, C5e, C6e}
<b>Growth Factor</b>	1.1127643944856531
<b>Reactions</b>	
R4	C3c dihydroxy acetone $\rightarrow$ C3b
R5	C1a formaldehyde + C3b $\rightarrow$ C4b
R7	C4b $\rightarrow$ C4c
R10	C1a formaldehyde + C4c $\rightarrow$ C5d
R12	C5d $\rightarrow$ C5e
R16	C1a formaldehyde + C5e $\rightarrow$ C6e
R37	C6e $\rightarrow$ C3b + C3c dihydroxy acetone

F.2. **E. coli.** Some details of the experiments on E. coli dataset are shown. A list of the compound names and their identifiers can be found in Table 16. The suffixes `_c` and `_e` represent that the molecules are internal or external to the cytoplasm, respectively. The reaction numbers shown in the following are arbitrarily assigned and can be ignored.

F.2.1. *Details of Figure 10.* The top 3 cores with the highest MGF in the E. coli dataset are the following:

F.2.2. *Details of Figure 13.* The result of Algorithm 3 on the E. coli dataset is:

The cores contained within it are found to be:

TABLE 6. Summary of the red core from Fig. 7.

Category	Details
<b>Food Set</b>	{C1a formaldehyde}
<b>Autocatalytic Set</b>	{C2a, C2b, C3a, C3b, C4a, C4b, C5a, C5b, C6a, C6b, C7b}
<b>Growth Factor</b>	1.1056824557955995
<b>Reactions</b>	
R1	$C2a \rightarrow C2b$
R2	$C1a \text{ formaldehyde} + C2b \rightarrow C3a$
R3	$C3a \rightarrow C3b$
R5	$C1a \text{ formaldehyde} + C3b \rightarrow C4b$
R6	$C4b \rightarrow C4a$
R8	$C1a \text{ formaldehyde} + C4a \rightarrow C5b$
R11	$C5b \rightarrow C5a$
R13	$C1a \text{ formaldehyde} + C5a \rightarrow C6a$
R17	$C6a \rightarrow C6b$
R20	$C1a \text{ formaldehyde} + C6b \rightarrow C7b$
R34	$C7b \rightarrow C2a + C5a$

TABLE 7. Summary of the green core from Fig. 10.

Category	Details
<b>Food Set</b>	{pep_c, h_e, glu_L_c, nh4_c}
<b>Waste Set</b>	{pyr_c, h2o_c, gln_L_c}
<b>Non-autocatalytic Set</b>	{adp_c}
<b>Autocatalytic Set</b>	{atp_c, h_c, pi_c}
<b>Growth Factor</b>	1.8932605011330286
<b>Reactions</b>	
R18	$adp_c + pi_c + 4h_e \rightarrow atp_c + 3h_c + h2o_c$
R20	$adp_c + h_c + pep_c \rightarrow atp_c + pyr_c$
R41	$atp_c + glu_L_c + nh4_c \rightarrow adp_c + h_c + pi_c + gln_L_c$

TABLE 8. Summary of the blue core from Fig. 10.

Category	Details
<b>Food Set</b>	{pep_c, h_e, gln_L_e}
<b>Waste Set</b>	{pyr_c, gln_L_c}
<b>Non-autocatalytic Set</b>	{adp_c, h2o_c}
<b>Autocatalytic Set</b>	{atp_c, h_c, pi_c}
<b>Growth Factor</b>	1.8932605011330286
<b>Reactions</b>	
R18	$adp_c + pi_c + 4h_e \rightarrow atp_c + 3h_c + h2o_c$
R20	$adp_c + h_c + pep_c \rightarrow atp_c + pyr_c$
R42	$atp_c + h2o_c + gln_L_e \rightarrow adp_c + h_c + pi_c + gln_L_c$

TABLE 9. Summary of the red core from Fig. 10.

Category	Details
Food Set	{pep_c, h_e}
Waste Set	{pyr_c}
Non-autocatalytic Set	{adp_c, h2o_c}
Autocatalytic Set	{atp_c, h_c, pi_c}
Growth Factor	1.8932605011330286
<b>Reactions</b>	
R13	$atp\_c + h2o\_c \rightarrow adp\_c + h\_c + pi\_c$
R18	$adp\_c + pi\_c + 4h\_e \rightarrow atp\_c + 3h\_c + h2o\_c$
R20	$adp\_c + h\_c + pep\_c \rightarrow atp\_c + pyr\_c$

TABLE 10. Summary of data from Algorithm 3 on the E. coli Dataset.

Category	Details
Growth Factor	2.7678080214824665
<b>Reactions</b>	
	$atp\_c + f6p\_c \rightarrow adp\_c + fdp\_c + h\_c$
	$atp\_c + oaa\_c \rightarrow adp\_c + co2\_c + pep\_c$
	$atp\_c + pyr\_c + h2o\_c \rightarrow 2h\_c + pep\_c + pi\_c + amp\_c$
	$atp\_c + amp\_c \rightarrow 2adp\_c$
	$adp\_c + pi\_c + 4h\_e \rightarrow atp\_c + 3h\_c + h2o\_c$
	$g3p\_c + s7p\_c \rightarrow f6p\_c + e4p\_c$
	$nadh\_c + 2h\_e + nadp\_c \rightarrow 2h\_c + nad\_c + nadph\_c$
	$dhap\_c \rightarrow g3p\_c$
	$fdp\_c \rightarrow g3p\_c + dhap\_c$
	$pep\_c + fru\_e \rightarrow f6p\_c + pyr\_c$
	$atp\_c + glu\_Lc + nh4\_c \rightarrow adp\_c + h\_c + pi\_c + gln\_Lc$
	$h\_c + akc\_c + gln\_Lc + nadph\_c \rightarrow 2glu\_Lc + nadp\_c$
	$nad\_c + mal\_Lc \rightarrow h\_c + nadh\_c + oaa\_c$

TABLE 11. Summary of Core 1 (Green) from Fig. 13.

Category	Details
Food Set	{nadh_c, akc_c, h_e, gln_Lc}
Waste Set	{nad_c, glu_Lc}
Non-autocatalytic Set	{nadph_c}
Autocatalytic Set	{h_c, nadp_c}
Growth Factor	1.4142011834319526
<b>Reactions</b>	
R7	$nadh\_c + 2h\_e + nadp\_c \rightarrow 2h\_c + nad\_c + nadph\_c$
R12	$h\_c + akc\_c + gln\_Lc + nadph\_c \rightarrow 2glu\_Lc + nadp\_c$

TABLE 12. Summary of Core 2 (Blue) from Fig. 13.

Category	Details
Food Set	{atp_c, akc_c, nadph_c, nh4_c}
Waste Set	{adp_c, pi_c, nadp_c}
Non-autocatalytic Set	{gln_L_c}
Autocatalytic Set	{h_c, glu_L_c}
Growth Factor	1.4142011834319526
<b>Reactions</b>	
R11	$\text{atp}_c + \text{glu}_L_c + \text{nh4}_c \rightarrow \text{adp}_c + \text{h}_c + \text{pi}_c + \text{gln}_L_c$
R12	$\text{h}_c + \text{akc}_c + \text{gln}_L_c + \text{nadph}_c \rightarrow 2\text{glu}_L_c + \text{nadp}_c$

TABLE 13. Summary of Core 3 (Orange) from Fig. 13.

Category	Details
Food Set	{pi_c, amp_c, h_e}
Waste Set	{h_c, h2o_c}
Autocatalytic Set	{adp_c, atp_c}
Growth Factor	1.4142011834319526
<b>Reactions</b>	
R4	$\text{atp}_c + \text{amp}_c \rightarrow 2\text{adp}_c$
R5	$\text{adp}_c + \text{pi}_c + 4\text{h}_e \rightarrow \text{atp}_c + 3\text{h}_c + \text{h2o}_c$

TABLE 14. Summary of Core 4 (Purple) from Fig. 13.

Category	Details
Food Set	{atp_c, s7p_c}
Waste Set	{adp_c, h_c, e4p_c}
Autocatalytic Set	{f6p_c, fdp_c, g3p_c, dhap_c}
Growth Factor	1.2207340620350884
<b>Reactions</b>	
R1	$\text{atp}_c + \text{f6p}_c \rightarrow \text{adp}_c + \text{fdp}_c + \text{h}_c$
R6	$\text{g3p}_c + \text{s7p}_c \rightarrow \text{f6p}_c + \text{e4p}_c$
R8	$\text{dhap}_c \rightarrow \text{g3p}_c$
R9	$\text{fdp}_c \rightarrow \text{g3p}_c + \text{dhap}_c$

TABLE 15. Summary of Core 5 (Yellow) from Fig. 13.

Category	Details
<b>Food Set</b>	{h_e, s7p_c, fru_e}
<b>Waste Set</b>	{h_c, amp_c, e4p_c, dhap_c}
<b>Non-autocatalytic Set</b>	{atp_c, pyr_c, pi_c}
<b>Autocatalytic Set</b>	{adp_c, f6p_c, fdp_c, h2o_c, pep_c, g3p_c}
<b>Growth Factor</b>	1.2207340620350884
<b>Reactions</b>	
R1	$\text{atp}_c + \text{f6p}_c \rightarrow \text{adp}_c + \text{fdp}_c + \text{h}_c$
R3	$\text{atp}_c + \text{pyr}_c + \text{h2o}_c \rightarrow 2\text{h}_c + \text{pep}_c + \text{pi}_c + \text{amp}_c$
R5	$\text{adp}_c + \text{pi}_c + 4\text{h}_e \rightarrow \text{atp}_c + 3\text{h}_c + \text{h2o}_c$
R6	$\text{g3p}_c + \text{s7p}_c \rightarrow \text{f6p}_c + \text{e4p}_c$
R9	$\text{fdp}_c \rightarrow \text{g3p}_c + \text{dhap}_c$
R10	$\text{pep}_c + \text{fru}_e \rightarrow \text{f6p}_c + \text{pyr}_c$



Identifier	Compound
adp_c	ADP C10H12N5O10P2
atp_c	ATP C10H12N5O13P3
f6p_c	D-Fructose 6-phosphate
fdp_c	D-Fructose 1
h_c	H+
accoa_c	Acetyl-CoA
coa_c	Coenzyme A
for_c	Formate
pyr_c	Pyruvate
g6p_c	D-Glucose 6-phosphate
13dpg_c	3-Phospho-D-glyceroyl phosphate
3pg_c	3-Phospho-D-glycerate
6pgc_c	6-Phospho-D-gluconate
6pgl_c	6-phospho-D-glucono-1
h2o_c	H2O H2O
acald_c	Acetaldehyde
nad_c	Nicotinamide adenine dinucleotide
nadh_c	Nicotinamide adenine dinucleotide - reduced
2pg_c	D-Glycerate 2-phosphate
etoh_c	Ethanol
ac_c	Acetate
actp_c	Acetyl phosphate
co2_c	CO2 CO2
oaa_c	Oxaloacetate
pep_c	Phosphoenolpyruvate
pi_c	Phosphate
acon_C_c	Cis-Aconitate
cit_c	Citrate
icit_c	Isocitrate
amp_c	AMP C10H12N5O7P
akg_c	2-Oxoglutarate
succoa_c	Succinyl-CoA
h_e	H+
e4p_c	D-Erythrose 4-phosphate
g3p_c	Glyceraldehyde 3-phosphate
gln_L_c	L-Glutamine
glu_L_c	L-Glutamate
nadp_c	Nicotinamide adenine dinucleotide phosphate
nadph_c	Nicotinamide adenine dinucleotide phosphate - reduced
r5p_c	Alpha-D-Ribose 5-phosphate
ru5p_D_c	D-Ribulose 5-phosphate
xu5p_D_c	D-Xylulose 5-phosphate
o2_c	O2 O2
q8_c	Ubiquinone-8
q8h2_c	Ubiquinol-8
fum_c	Fumarate

TABLE 16. Table of identifier and compound names for the E. coli dataset.

<b>Identifier</b>	<b>Compound</b>
succ_c	Succinate
s7p_c	Sedoheptulose 7-phosphate
dhap_c	Dihydroxyacetone phosphate
fru_e	D-Fructose
mal_L_c	L-Malate
glc_D_e	D-Glucose
nh4_c	Ammonium
gln_L_e	L-Glutamine
glx_c	Glyoxylate
lac_D_c	D-Lactate

TABLE 17. Table of identifier and compound names for the E. coli dataset. (Cont.)